Ann. Telecommun. (2010) 65:391–410
DOI 10.1007/s12243-010-0169-z

Mobile-to-mobile fading channels in amplify-and-forward relay systems under line-of-sight conditions: statistical modeling and analysis

Batool Talha · Matthias Pätzold

Received: 13 July 2009 / Accepted: 18 March 2010 / Published online: 29 April 2010

Abstract This paper deals with the modeling and analysis of narrowband mobile-to-mobile (M2M) fading channels for amplify-and-forward relay links under line-of-sight (LOS) conditions. It is assumed that a LOS component exists in the direct link between the source mobile station (SMS) and the destination mobile station (DMS), as well as in the links via the mobile relay (MR). The proposed channel model is referred to as the multiple-LOS second-order scattering (MLSS) channel model. The MLSS channel model is derived from a second-order scattering process, where the received signal is modeled in the complex baseband as the sum of a single and a double scattered component. Analytical expressions are derived for the mean value, variance, probability density function (PDF), cumulative distribution function (CDF), level-crossing rate (LCR), and average duration of fades (ADF) of the received envelope of MLSS channels. The PDF of the channel phase is also investigated. It is observed that the LOS components and the relay gain have a significant influence on the statistics of MLSS channels. It is also shown that MLSS channels include various other channel models as special cases, e.g., double Rayleigh channels, double Rice channels, single-LOS double-scattering (SLDS) channels, non-line-of-sight (NLOS) second-order scattering (NLSS) channels, and single-LOS second-order scattering (SLSS) channels. The correctness of all analytical results is confirmed by simulations using a high performance channel simulator. Our novel MLSS channel model is of significant importance for the system level performance evaluation of M2M communication systems in different M2M propagation scenarios. Furthermore, our studies pertaining to the fading behavior of MLSS channels are useful for the design and development of relay-based cooperative wireless networks.

Keywords Amplify-and-forward relay systems · Mobile-to-mobile fading channels · Double Rayleigh process · Double Rice process · Probability density function · Level-crossing rate · Average duration of fades

1 Introduction

Among several upcoming new wireless technologies, M2M communication [1] in cooperative networks has gained considerable attention in recent years. The driving force behind merging M2M communication into cooperative networks is its promise to provide a better link quality (higher diversity gain), an improved network range, and an overall increase in the system capacity. M2M cooperative wireless networks exploit the fact that single-antenna mobile stations cooperate with each other to share their antennas in order to form a virtual multiple-input multiple-output (MIMO) system

The material in this paper was presented in part at the 19th IEEE International Symposium on Personal, Indoor and Mobile Radio Communications, PIMRC 2008, Cannes, France, September 2008.

The material in this paper has been published in part in the proceedings of the 51st IEEE Globecom 2008, New Orleans, USA, December 2008.

B. Talha (✉) · M. Pätzold
University of Agder, Grimstad, Norway
e-mail: batool.talha@uia.no

M. Pätzold
e-mail: matthias.paetzold@uia.no

in a multi-user scenario [2]. Thus, in such networks, cooperative diversity [3–6] is achieved by relaying the signal transmitted from a mobile station to the final destination using other mobile stations in the network. However, to cope with the problems faced within the development of such systems, a solid knowledge of the underlying multipath fading channel characteristics is essential.

M2M fading channels in cooperative networks can be modeled as a sum of multiplicative fading channels. This sum of multiplicative fading channels is also called the multiple scattering radio propagation channel [7]. In a multiple scattering radio propagation environment, the received signal is composed of single, double, and in general multiple scattered components [7]. The multiple scattering concept provides a starting point for modeling the signal envelope fluctuations of various types of M2M channels, so that their statistical properties are in good agreement with measurement data [7–9]. In terms of statistics, M2M fading channels for relay-based cooperative networks are usually characterized by the mean, variance, and probability density function (PDF) of the envelope and phase of the received signal. Unfortunately, the envelope and phase distributions do not provide any information pertaining to the rate of fading of the channel. However, a detailed knowledge of the fading behavior of M2M fading channels is indispensable to the development, performance analysis, and test of cooperative wireless networks. The LCR of the envelope of fading channels is an important statistical quantity, revealing information about how fast the received signal changes with time. It is basically a measure to describe the average number of times the signal envelope crosses a certain threshold level from up to down (or from down to up) per second. Another important statistical quantity is the ADF, which is defined as the expected value of the time intervals over which the fading signal envelope remains below a certain threshold level.

Studies pertaining to the statistical properties of M2M fading channels under NLOS propagation conditions in non-cooperative single-input single-output (SISO) systems can be found in [1, 10]. Real-world measurement data for narrowband M2M fading channels are studied in [11]. Analysis of correlation properties in the form of autocorrelation functions (ACFs) and cross-correlation functions (CCFs) for M2M fading channels in non-cooperative MIMO systems are available in [12, 13]. A variety of M2M propagation scenarios in relay-based cooperative networks however exists. Several models have therefore been proposed so far to characterize the fading statistics of M2M fading channels in such networks. Under NLOS propagation conditions, the M2M amplify-and-forward relay fading channel can be modeled as a double Rayleigh process [8, 9, 14]. Experimental measurements of outdoor-to-indoor M2M fading channels analyzed in [9] provide us with a solid ground to believe that double Rayleigh processes are well suited to model such channels. A detailed analysis on the statistics of double Rayleigh channels is presented in [14]. The authors of [15] have addressed the impact of double Rayleigh fading on the systems performance. Furthermore, motivated by the studies of double Rayleigh fading channels for keyhole channels [16], the so-called double Nakagami-m and cascaded Weibull fading channels have been proposed in [17] and [18], respectively. From the physical point of view it is reasonable to extend the double Rayleigh channel model to the double Rice channel model for M2M amplify-and-forward relay fading channels under LOS propagations conditions [19]. The double Rice channels come into play when LOS components exist in the transmission links from the SMS to the DMS via the relay. A thorough study pertaining to the dynamic behavior of double Rice channels is presented in [19]. In amplify-and-forward relay systems, profiting from cooperative diversity schemes requires a further extension of the double Rayleigh channel model by adding a direct link from the SMS to the DMS. The resulting channel, obtained by combining the SMS-MR-DMS link and the SMS-DMS link is named as the NLSS channel model. The signal received after traversing through NLSS channels is composed of a sum of a single and a double scattered component [20, 21]. Studies conducted for NLSS channels provide us with a thorough analysis of the PDF and CDF of NLSS channels. However, there is a lack of information regarding the LCR and ADF of NLSS channels in the literature. The extension of NLSS fading channel models, when a significant LOS component is present between the direct SMS-DMS link, results in SLSS channels [20, 21]. SLSS channels have only been partially analyzed so far just as NLSS channels. A detailed analysis of the statistical properties of a physically non-realistic channel called the SLDS channel is presented in [22]. SLDS channel models can not be justified physically, since the scattered component of the direct SMS-DMS link is ignored while modeling the M2M fading channels.

In this paper, we propose a novel channel model referred to as the MLSS fading channel for amplify-and-forward relay channels under LOS conditions [23]. This model is specifically developed for such relay-based cooperative networks where time-division multiple-access (TDMA) based amplify-and-forward relay protocols [24–26] are employed. Furthermore, MLSS fading channels belong to the class of second-order

scattering channels, where the received signal is modeled in the complex baseband as a sum of the single and the double scattered component. We have assumed that a LOS component is present in the direct link between the SMS and the DMS (i.e., the SMS-DMS link) as well as in the two links via the MR (i.e., the SMS-MR link and the MR-DMS link). For this new class of MLSS channels, we derive analytical expressions for the mean value, variance, PDF, CDF, LCR, and ADF of the received envelope as well as for the PDF of the channel phase assuming isotropic scattering conditions. We also show that the derived analytical expressions for MLSS processes include the corresponding expressions for double Rayleigh, double Rice, SLDS, NLSS, and SLSS processes as special cases. The correctness of all analytical results is confirmed by simulations using a high-performance channel simulator. Notice that problems pertaining to the protocol level and system level implementation of amplify-and-forward relay networks are out of scope of the current paper. However, the analytical results presented in this article are important for the development and performance evaluation of relay-based cooperative networks in different M2M propagation environments under LOS and NLOS conditions.

The rest of the paper is structured as follows: In Section 2, the reference model for amplify-and-forward MLSS fading channels is developed. Section 3 deals with the analysis of the statistical properties of MLSS fading processes. Special cases of MLSS fading channels are discussed in detail in Section 4. Section 5 confirms the validity of the analytical expressions presented in Section 3 by simulations. Finally, concluding remarks are given in Section 6.

2 The MLSS fading channel

Taking into consideration the limitations on the physical implementation of the mobile stations, i.e., the SMS, the mobile relay, and the DMS in an amplify-and-forward relay communication system, the mentioned mobile stations mostly operate in half-duplex. This means that the mobile stations cannot transmit and receive a signal in the same frequency band at the same time. Here, it is assumed that the SMS continuously communicates with the DMS, i.e., the signal transmitted by the SMS in each time slot is received by the DMS. The MR, however, receives a signal from the SMS in the first time slot and re-transmits it to the DMS in the second time slot [24–26]. The considered communication scenario determined by an SMS, a DMS, and an MR is shown in Fig. 1.

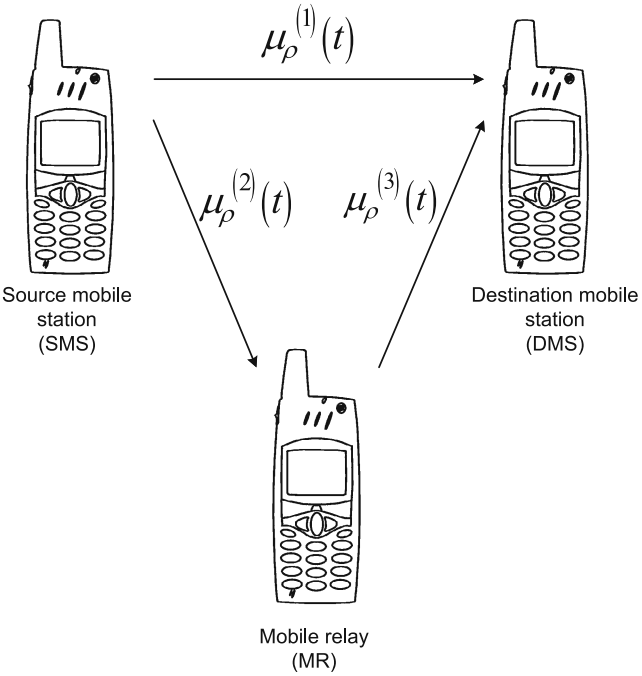

Fig. 1 The propagation scenario describing MLSS fading channels

In general, under NLOS conditions, the complex time-varying channel gain of the multiple scattering radio propagation channel proposed in [7] can be written as

$$\chi(t) = \alpha_1 \mu^{(1)}(t) + \alpha_2 \mu^{(2)}(t)\,\mu^{(3)}(t) + \alpha_3 \mu^{(4)}(t)\,\mu^{(5)}(t)\,\mu^{(6)}(t) + \cdots \quad (1)$$

where $\mu^{(i)}(t)$ $(i = 1, 2, 3, \ldots)$ is a zero-mean complex Gaussian process that represents the scattered component of the ith link and α_i $(i = 1, 2, 3, \ldots)$ is a real-valued constant that determines the contribution of the ith scattered component. In (1), the Gaussian processes $\mu^{(i)}(t)$ are mutually independent. However, when the fading channel is modeled by taking into account only the first two terms of (1), the resulting channel is referred to as the NLSS channel [20, 21]. Here, we are presenting an extension of the NLSS channel to the MLSS channel by incorporating a LOS component in all transmission links.

Starting from (1), ignoring $\mu^{(i)}(t)$ $\forall\, i \geq 4$, and replacing $\mu^{(i)}(t)$ by $\mu_\rho^{(i)}(t)$ for $i = 1, 2, 3$, results in

$$\chi_\rho(t) = \mu_\rho^{(1)}(t) + A_{\mathrm{MR}}\,\mu_\rho^{(2)}(t)\,\mu_\rho^{(3)}(t) \quad (2)$$

where $\alpha_1 = 1$ and $\alpha_2 = A_{\mathrm{MR}}$. The signal model in (2) represents well the considered propagation scenario, where the direct transmission link from the SMS to the DMS and the link via the MR coexist every second time slot.

In (2), the quantity A_{MR} is called the relay gain, which is a real constant quantity. In (2), $\mu_{\rho}^{(1)}(t)$, $\mu_{\rho}^{(2)}(t)$, and $\mu_{\rho}^{(3)}(t)$ are statistically independent non-zero-mean complex Gaussian processes, which model the subchannels in the SMS-DMS, SMS-MR, and MR-DMS links, respectively (see Fig. 1). Each complex Gaussian process $\mu_{\rho}^{(i)}(t) = \mu_{\rho_1}^{(i)}(t) + j\mu_{\rho_2}^{(i)}(t)$ represents the sum of a scattered component $\mu^{(i)}(t)$ and a LOS component $m^{(i)}(t)$, i.e., $\mu_{\rho}^{(i)}(t) = \mu^{(i)}(t) + m^{(i)}(t)$. The scattered component $\mu^{(i)}(t) = \mu_1^{(i)}(t) + j\mu_2^{(i)}(t)$ is modeled by a zero-mean complex Gaussian process with variance $2\sigma_i^2$. Furthermore, the power spectral density (PSD) $S_{\mu^{(i)}\mu^{(i)}}(f)$ can be proved to be symmetrical for isotropic scattering conditions [27]. The LOS component $m^{(i)}(t) = \rho_i e^{j(2\pi f_{\rho_i} t + \theta_{\rho_i})}$ assumes a fixed amplitude ρ_i, a constant Doppler frequency f_{ρ_i}, and a constant phase θ_{ρ_i} for $i = 1, 2, 3$. Let us denote the second term in (2), which is a weighted non-zero-mean complex double Gaussian process, as $\varsigma_{\rho}(t) = \varsigma_{\rho_1}(t) + j\varsigma_{\rho_2}(t) = A_{\mathrm{MR}}\,\mu_{\rho}^{(2)}(t)\,\mu_{\rho}^{(3)}(t)$. From Fig. 1, we can realize that $\varsigma_{\rho}(t)$ models the overall fading in the SMS-MR-DMS link. It is worth mentioning here that the relay gain A_{MR} is just a scaling factor for the mean and variance of the complex Gaussian process $\mu_{\rho}^{(3)}(t)$, i.e., $m^{(3)}(t) = E\{A_{\mathrm{MR}}\,\mu_{\rho}^{(3)}(t)\} = \rho_{A_{\mathrm{MR}}} e^{j(2\pi f_{\rho_3} t + \theta_{\rho_3})}$, where $\rho_{A_{\mathrm{MR}}} = A_{\mathrm{MR}}\,\rho_3$ and $2\sigma_{A_{\mathrm{MR}}}^2 = \mathrm{Var}\{A_{\mathrm{MR}}\,\mu_{\rho}^{(3)}(t)\} = 2\,(A_{\mathrm{MR}}\,\sigma_3)^2$. Finally, the overall fading process that takes into account the direct SMS-DMS link and the SMS-DMS link via the MR results in the complex process $\chi_{\rho}(t) = \chi_{\rho_1}(t) + j\chi_{\rho_2}(t)$ introduced in (2). The absolute value of $\chi_{\rho}(t)$ defines the MLSS process

$$\Xi(t) = |\chi_{\rho}(t)| = |\mu_{\rho}^{(1)}(t) + \varsigma_{\rho}(t)|. \tag{3}$$

Furthermore, the argument of $\chi_{\rho}(t)$ introduces the phase process $\Theta(t)$

$$\Theta(t) = \arg\{\chi_{\rho}(t)\}. \tag{4}$$

It is important to point out here that the signal reaching the DMS via the mobile relay is delayed by one time slot. However, we have not introduced this time delay in (2). One of the reasons behind this is that the time delay is meaningless in channel modeling and system performance analysis. Notice, a time delay only introduces a phase shift in the signal. Thus, this delay does not affect the envelope related statistical properties of the channel, like for example, PDF, LCR, and ADF. Besides, it is assumed that the subchannels in the SMS-DMS, SMS-MR, and MR-DMS links are uncorrelated (see Section 3). It can be shown that the correlation properties of a channel, such as the cross-correlation function (CCF), are independent of the time delay. Meaning thereby, the observed delay here would not influence the correlation properties of the overall channel.

If there is no delay, then the received signal is like a superposition of different multipath components. These multipath components can be single-, double-, triple-scattered components as shown in [7]. In our system, the transmitted signal arrives at the DMS after crossing two links. One of the links can be modeled as a single scattered component and the other link corresponds to a double scattered component. The superposition of the multipath components is given in (2).

3 Analysis of MLSS fading channels

In this section, we analyze the statistical properties of MLSS fading channels introduced in Section 2. The starting point for the derivation of the analytical expressions of the most important statistical quantities like the mean value, variance, PDF, LCR, and ADF of MLSS fading channels, as well as the PDF of the corresponding phase process is the computation of the joint PDF $p_{\chi_{\rho_1}\chi_{\rho_2}\dot{\chi}_{\rho_1}\dot{\chi}_{\rho_2}}(u_1, u_2, \dot{u}_1, \dot{u}_2; t)$ of the stochastic processes $\chi_{\rho_1}(t)$, $\chi_{\rho_2}(t)$, $\dot{\chi}_{\rho_1}(t)$, and $\dot{\chi}_{\rho_2}(t)$ at the same time t. Throughout this paper, the overdot indicates the time derivative. The joint PDF $p_{\chi_{\rho_1}\chi_{\rho_2}\dot{\chi}_{\rho_1}\dot{\chi}_{\rho_2}}(u_1, u_2, \dot{u}_1, \dot{u}_2; t)$ can be expressed in terms of a 4-dimensional (4D) convolution integral as

$$\begin{aligned} &p_{\chi_{\rho_1}\chi_{\rho_2}\dot{\chi}_{\rho_1}\dot{\chi}_{\rho_2}}(u_1, u_2, \dot{u}_1, \dot{u}_2; t) \\ &\quad = \int_{-\infty}^{\infty}\int_{-\infty}^{\infty}\int_{-\infty}^{\infty}\int_{-\infty}^{\infty} d\dot{y}_2\, d\dot{y}_1\, dy_2\, dy_1\; p_{\varsigma_{\rho_1}\varsigma_{\rho_2}\dot{\varsigma}_{\rho_1}\dot{\varsigma}_{\rho_2}\mu_{\rho_1}^{(1)}\mu_{\rho_2}^{(1)}\dot{\mu}_{\rho_1}^{(1)}\dot{\mu}_{\rho_2}^{(1)}} \\ &\qquad \times (y_1, y_2, \dot{y}_1, \dot{y}_2, u_1 - y_1, u_2 - y_2, \\ &\qquad\quad \dot{u}_1 - \dot{y}_1, \dot{u}_2 - \dot{y}_2; t) \end{aligned} \tag{5}$$

where $p_{\varsigma_{\rho_1}\varsigma_{\rho_2}\dot{\varsigma}_{\rho_1}\dot{\varsigma}_{\rho_2}\mu_{\rho_1}^{(1)}\mu_{\rho_2}^{(1)}\dot{\mu}_{\rho_1}^{(1)}\dot{\mu}_{\rho_2}^{(1)}}(y_1, y_2, \dot{y}_1, \dot{y}_2, u_1, u_2, \dot{u}_1, \dot{u}_2; t)$ is the joint PDF of the processes $\mu_{\rho_1}^{(1)}(t)$, $\mu_{\rho_2}^{(1)}(t)$, $\dot{\mu}_{\rho_1}^{(1)}(t)$, $\dot{\mu}_{\rho_2}^{(1)}(t)$, $\varsigma_{\rho_1}(t)$, $\varsigma_{\rho_2}(t)$, $\dot{\varsigma}_{\rho_1}(t)$, and $\dot{\varsigma}_{\rho_2}(t)$ at the same time t. It is important to note that the processes $\mu_{\rho_i}^{(1)}(t)$, $\dot{\mu}_{\rho_i}^{(1)}(t)$, $\varsigma_{\rho_i}(t)$, and $\dot{\varsigma}_{\rho_i}(t)$ $(i = 1, 2)$ are mutually uncorrelated.[1] Furthermore, the statistically independent nature of the process pairs $\{\mu_{\rho_i}^{(1)}(t), \dot{\mu}_{\rho_i}^{(1)}(t)\}$ and $\{\varsigma_{\rho_i}(t), \dot{\varsigma}_{\rho_i}(t)\}$

[1] The PSD $S_{\mu^{(i)}\mu^{(i)}}(f)$ is an even function. Then, $\mu^{(i)}(t)$ and $\dot{\mu}^{(i)}(t)$ are uncorrelated at the same point in time, because $r_{\mu^{(i)}\dot{\mu}^{(i)}}(0) = -\frac{d}{d\tau} r_{\mu^{(i)}\mu^{(i)}}(\tau)\,|_0 = -j2\pi \int_{-\infty}^{\infty} f\, S_{\mu^{(i)}\mu^{(i)}}(f)\, d\tau = 0$. Since, $\mu^{(i)}(t)$ and $\dot{\mu}^{(i)}(t)$ are uncorrelated Gaussian processes, it follows that $\mu^{(i)}(t)$ and $\dot{\mu}^{(i)}(t)$ are also independent [28].

$(i=1,2)$ allows us to write $p_{\varsigma_{\rho_1}\varsigma_{\rho_2}\dot{\varsigma}_{\rho_1}\dot{\varsigma}_{\rho_2}\mu_{\rho_1}^{(1)}\mu_{\rho_2}^{(1)}\dot{\mu}_{\rho_1}^{(1)}\dot{\mu}_{\rho_2}^{(1)}}\left(y_1, y_2, \dot{y}_1, \dot{y}_2, u_1, u_2, \dot{u}_1, \dot{u}_2; t\right)$ as a product of the joint PDFs $p_{\mu_{\rho_1}^{(1)}\mu_{\rho_2}^{(1)}\dot{\mu}_{\rho_1}^{(1)}\dot{\mu}_{\rho_2}^{(1)}}(u_1, u_2, \dot{u}_1, \dot{u}_2; t)$ and $p_{\varsigma_{\rho_1}\varsigma_{\rho_2}\dot{\varsigma}_{\rho_1}\dot{\varsigma}_{\rho_2}}\left(y_1, y_2, \dot{y}_1, \dot{y}_2; t\right)$. Hence, (5) becomes

$$
\begin{aligned}
&p_{\chi_{\rho_1}\chi_{\rho_2}\dot{\chi}_{\rho_1}\dot{\chi}_{\rho_2}}(u_1, u_2, \dot{u}_1, \dot{u}_2; t)\\
&= \int_{-\infty}^{\infty}\int_{-\infty}^{\infty}\int_{-\infty}^{\infty}\int_{-\infty}^{\infty} d\dot{y}_2\, d\dot{y}_1\, dy_2\, dy_1\; p_{\varsigma_{\rho_1}\varsigma_{\rho_2}\dot{\varsigma}_{\rho_1}\dot{\varsigma}_{\rho_2}}\\
&\quad\times(y_1, y_2, \dot{y}_1, \dot{y}_2; t)\; p_{\mu_{\rho_1}^{(1)}\mu_{\rho_2}^{(1)}\dot{\mu}_{\rho_1}^{(1)}\dot{\mu}_{\rho_2}^{(1)}}\\
&\quad\times(u_1 - y_1, u_2 - y_2, \dot{u}_1 - \dot{y}_1, \dot{u}_2 - \dot{y}_2; t) \qquad (6)
\end{aligned}
$$

where $p_{\mu_{\rho_1}^{(1)}\mu_{\rho_2}^{(1)}\dot{\mu}_{\rho_1}^{(1)}\dot{\mu}_{\rho_2}^{(1)}}(u_1, u_2, \dot{u}_1, \dot{u}_2; t)$ is the joint PDF of the processes $\mu_{\rho_i}^{(1)}(t)$ and $\dot{\mu}_{\rho_i}^{(1)}(t)$ $(i=1,2)$ at the same time t. Using the multivariate Gaussian distribution (see, e.g., [29, Eq. (3.2)]), this joint PDF can be written as in (8). Similarly, $p_{\varsigma_{\rho_1}\varsigma_{\rho_2}\dot{\varsigma}_{\rho_1}\dot{\varsigma}_{\rho_2}}(y_1, y_2, \dot{y}_1, \dot{y}_2; t)$ in (6), represents the joint PDF of the processes $\varsigma_{\rho_i}(t)$ and $\dot{\varsigma}_{\rho_i}(t)$ $(i=1,2)$ at the same time t. Recall that the stochastic process $\varsigma_\rho(t)$ is a product process, i.e., $\varsigma_\rho(t) = A_{\mathrm{MR}}\,\mu_\rho^{(2)}(t)\,\mu_\rho^{(3)}(t)$. Thus, exploiting the statistical independent nature of the underlying complex Gaussian processes, i.e., $\mu_\rho^{(2)}(t)$ and $\mu_\rho^{(3)}(t)$, we can write the joint PDF $p_{\varsigma_{\rho_1}\varsigma_{\rho_2}\dot{\varsigma}_{\rho_1}\dot{\varsigma}_{\rho_2}}(y_1, y_2, \dot{y}_1, \dot{y}_2; t)$ as follows

$$
\begin{aligned}
&p_{\varsigma_{\rho_1}\varsigma_{\rho_2}\dot{\varsigma}_{\rho_1}\dot{\varsigma}_{\rho_2}}(y_1, y_2, \dot{y}_1, \dot{y}_2; t)\\
&= \int_{-\infty}^{\infty}\int_{-\infty}^{\infty}\int_{-\infty}^{\infty}\int_{-\infty}^{\infty} d\dot{z}_2\, d\dot{z}_1\, dz_2\, dz_1\, |J|^{-1} p_{\mu_{\rho_1}^{(2)}\mu_{\rho_2}^{(2)}\dot{\mu}_{\rho_1}^{(2)}\dot{\mu}_{\rho_2}^{(2)}}\\
&\quad\times(z_1, z_2, \dot{z}_1, \dot{z}_2; t)\; p_{\mu_{\rho_1}^{(3)}\mu_{\rho_2}^{(3)}\dot{\mu}_{\rho_1}^{(3)}\dot{\mu}_{\rho_2}^{(3)}}\left(\frac{y_1}{z_1}, \frac{y_2}{z_2}, \frac{\dot{y}_1}{\dot{z}_1}, \frac{\dot{y}_2}{\dot{z}_2}; t\right) \qquad (7)
\end{aligned}
$$

where $|J| = (z_1^2 + z_2^2)^2$ denotes the Jacobian determinant and $p_{\mu_{\rho_1}^{(i)}\mu_{\rho_2}^{(i)}\dot{\mu}_{\rho_1}^{(i)}\dot{\mu}_{\rho_2}^{(i)}}(z_1, z_2, \dot{z}_1, \dot{z}_2; t)$ $(i=2,3)$ is the multivariate Gaussian distribution [29, Eq. (3.2)]. The solution of (7) is presented in (9).

$$
\begin{aligned}
&p_{\mu_{\rho_1}^{(1)}\mu_{\rho_2}^{(1)}\dot{\mu}_{\rho_1}^{(1)}\dot{\mu}_{\rho_2}^{(1)}}(u_1, u_2, \dot{u}_1, \dot{u}_2; t)\\
&= \frac{1}{(2\pi)^2\sigma_1^2\beta_1} e^{-\frac{\left(u_1 - m_1^{(1)}(t)\right)^2 + \left(u_2 - m_2^{(1)}(t)\right)^2}{2\sigma_1^2}} e^{-\frac{\left(\dot{u}_1 - \dot{m}_1^{(1)}(t)\right)^2 + \left(\dot{u}_2 - \dot{m}_2^{(1)}(t)\right)^2}{2\beta_1}}. \qquad (8)
\end{aligned}
$$

$$
\begin{aligned}
&p_{\varsigma_{\rho_1}\varsigma_{\rho_2}\dot{\varsigma}_{\rho_1}\dot{\varsigma}_{\rho_2}}(y_1, y_2, \dot{y}_1, \dot{y}_2; t)\\
&= \int_{-\infty}^{\infty}\int_{-\infty}^{\infty} dz_2\, dz_1 \frac{e^{-\frac{\left(z_1 - m_1^{(3)}(t)\right)^2 + \left(z_2 - m_2^{(3)}(t)\right)^2}{2\sigma_{A_{\mathrm{MR}}}^2}} e^{-\frac{\left(\dot{m}_1^{(3)}(t)\right)^2 + \left(\dot{m}_2^{(3)}(t)\right)^2}{2\beta_3}}}{(2\pi)^3\sigma_2^2\sigma_{A_{\mathrm{MR}}}^2\left[\beta_3\left(y_1^2 + y_2^2\right) + \beta_2\left(z_1^2 + z_2^2\right)^2\right]} e^{\frac{\beta_2\left(z_1^2+z_2^2\right)^2\left\{\left(\dot{m}_1^{(3)}(t)\right)^2 + \left(\dot{m}_2^{(3)}(t)\right)^2\right\} + \beta_3\left(y_1^2+y_2^2\right)\left(\dot{m}_1^{(2)}(t) + \dot{m}_2^{(2)}(t)\right)}{2\beta_2\left\{\beta_3\left(y_1^2+y_2^2\right) + \beta_2\left(z_1^2+z_2^2\right)^2\right\}}}\\
&\quad\times e^{-\frac{y_1^2+y_2^2-2\left(y_2 m_2^{(2)}(t) + y_1 m_1^{(2)}(t)\right)z_1 - 2\left(y_2 m_2^{(2)}(t) - y_1 m_2^{(2)}(t)\right)z_2 + \left\{\left(m_1^{(2)}(t)\right)^2 + \left(m_2^{(2)}(t)\right)^2\right\}\left(z_1^2+z_2^2\right)}{2\sigma_2^2\left(z_1^2+z_2^2\right)}} e^{\frac{z_1\dot{m}_2^{(3)}(t)\left(-y_2\dot{y}_1 + y_1\dot{y}_2 - \dot{m}_2^{(2)}(t)y_1 z_1 + \dot{m}_1^{(2)}(t)y_2 z_1\right)}{\beta_3\left(y_1^2+y_2^2\right) + \beta_2\left(z_1^2+z_2^2\right)^2}}\\
&\quad\times e^{-\frac{\dot{y}_1^2+\dot{y}_2^2-2\left(\dot{y}_2 \dot{m}_2^{(2)}(t) + \dot{y}_1 \dot{m}_1^{(2)}(t)\right)z_1 - 2\left(\dot{y}_2 \dot{m}_1^{(2)}(t) - \dot{y}_1 \dot{m}_2^{(2)}(t)\right)z_2 + \left\{\left(\dot{m}_1^{(2)}(t)\right)^2 + \left(\dot{m}_2^{(2)}(t)\right)^2\right\}\left(z_1^2+z_2^2\right)}{2\beta_2\left(z_1^2+z_2^2\right)}} e^{\frac{z_1\dot{m}_1^{(3)}(t)\left(y_1\dot{y}_1 + y_2\dot{y}_2 - \dot{m}_2^{(2)}(t)y_1 z_1 + \dot{m}_2^{(2)}(t)y_2 z_1\right)}{\beta_3\left(y_1^2+y_2^2\right) + \beta_2\left(z_1^2+z_2^2\right)^2}}\\
&\quad\times e^{\frac{2\beta_2 z_2\left(z_1^2+z_2^2\right)\left\{\dot{m}_1^{(3)}(t)\left(y_2\dot{y}_1 - y_1\dot{y}_2 + 2\dot{m}_2^{(2)}(t)y_1 z_1 - 2\dot{m}_1^{(2)}(t)y_2 z_1\right) + \dot{m}_2^{(3)}(t)\left(y_1\dot{y}_1 + y_2\dot{y}_2 - 2\dot{m}_1^{(2)}(t)y_1 z_1 - 2\dot{m}_2^{(2)}(t)y_2 z_1\right)\right\} + \beta_3\left(y_1^2+y_2^2\right)\left(\dot{y}_1^2+\dot{y}_2^2\right)}{2\beta_2\left(z_1^2+z_2^2\right)\left\{\beta_3\left(y_1^2+y_2^2\right) + \beta_2\left(z_1^2+z_2^2\right)^2\right\}}}\\
&\quad\times e^{\frac{z_2^2\left\{\dot{m}_1^{(2)}(t)\dot{m}_1^{(3)}(t)y_1 + \dot{m}_2^{(2)}(t)\dot{m}_2^{(3)}(t)y_1 + \dot{m}_2^{(2)}(t)\dot{m}_1^{(3)}(t)y_2 - \dot{m}_1^{(2)}(t)\dot{m}_2^{(3)}(t)y_2\right\}}{\beta_3\left(y_1^2+y_2^2\right) + \beta_2\left(z_1^2+z_2^2\right)^2}} e^{\frac{\beta_3\left(y_1^2+y_2^2\right)\left[-2\dot{y}_2\left(\dot{m}_2^{(2)}(t)z_1 + \dot{m}_1^{(2)}(t)z_2\right) + 2\dot{y}_1\left(-\dot{m}_1^{(2)}(t)z_1 + \dot{m}_2^{(2)}(t)z_2\right)\right]}{2\beta_2\left(z_1^2+z_2^2\right)\left\{\beta_3\left(y_1^2+y_2^2\right) + \beta_2\left(z_1^2+z_2^2\right)^2\right\}}}. \qquad (9)
\end{aligned}
$$

It should be pointed out here that the joint densities $p_{\mu_{\rho_1}^{(1)}\mu_{\rho_2}^{(1)}\dot{\mu}_{\rho_1}^{(1)}\dot{\mu}_{\rho_2}^{(1)}}(u_1, u_2, \dot{u}_1, \dot{u}_2; t)$ and $p_{\varsigma_{\rho_1}\varsigma_{\rho_2}\dot{\varsigma}_{\rho_1}\dot{\varsigma}_{\rho_2}}\left(y_1, y_2, \dot{y}_1, \dot{y}_2; t\right)$ are functions of time t because of the Doppler frequency f_{ρ_i} of the LOS component $m^{(i)}(t)$ $(i=1,2,3)$. Only for the special case when $f_{\rho_i} = 0\,\forall\, i = 1,2,3$, the joint densities $p_{\mu_{\rho_1}^{(1)}\mu_{\rho_2}^{(1)}\dot{\mu}_{\rho_1}^{(1)}\dot{\mu}_{\rho_2}^{(1)}}(u_1, u_2, \dot{u}_1, \dot{u}_2)$ and $p_{\varsigma_{\rho_1}\varsigma_{\rho_2}\dot{\varsigma}_{\rho_1}\dot{\varsigma}_{\rho_2}}(y_1, y_2, \dot{y}_1, \dot{y}_2)$ become independent of time t. Furthermore, in (8) and (9), the quantity β_i $(i=1,2,3)$ is the negative curvature of the autocorrelation function of the inphase and quadrature components of $\mu^{(i)}(t)$ $(i=1,2,3)$. Under isotropic scattering conditions, the quantities β_i $(i=1,2,3)$ can be expressed for M2M fading channels as [10, 30]

$$\beta_1 = 2(\sigma_1\pi)^2\left(f_{\mathrm{SMS}_{\max}}^2 + f_{\mathrm{DMS}_{\max}}^2\right) \qquad (10a)$$

$$\beta_2 = 2(\sigma_2\pi)^2\left(f_{\mathrm{SMS}_{\max}}^2 + f_{\mathrm{MR}_{\max}}^2\right) \qquad (10b)$$

$$\beta_3 = 2\left(\sigma_{A_{\mathrm{MR}}}\pi\right)^2\left(f_{\mathrm{MR}_{\max}}^2 + f_{\mathrm{DMS}_{\max}}^2\right) \qquad (10c)$$

where the symbols $f_{\mathrm{SMS}_{\max}}$, $f_{\mathrm{MR}_{\max}}$, and $f_{\mathrm{DMS}_{\max}}$ denote the maximum Doppler frequency caused by the motion of the SMS, the MR, and the DMS, respectively. Note

that the maximum Doppler frequencies associated with the individual M2M subchannels in the SMS-DMS, SMS-MR, and MR-DMS links, i.e., $f_{\text{SMS-DMS}_{\max}}$, $f_{\text{SMS-MR}_{\max}}$, and $f_{\text{MR-DMS}_{\max}}$ are greater than maximum Doppler frequencies $f_{\text{SMS}_{\max}}$, $f_{\text{MR}_{\max}}$, and $f_{\text{DMS}_{\max}}$. Substituting (8) and (9) in (6), applying the concept of transformation of random variables [28], and doing tedious algebraic manipulations, allow us to express the joint PDF $p_{\Xi\dot{\Xi}\Theta\dot{\Theta}}\left(x,\dot{x},\theta,\dot{\theta};t\right)$ of the MLSS process $\Xi(t)$, and the phase process $\Theta(t)$ as well as their respective time derivatives $\dot{\Xi}(t)$ and $\dot{\Theta}(t)$ as shown in (11). The resulting joint PDF $p_{\Xi\dot{\Xi}\Theta\dot{\Theta}}\left(x,\dot{x},\theta,\dot{\theta};t\right)$ is of fundamental importance, because it provides the basis for the computation of the PDF, LCR, and ADF of MLSS processes $\Xi(t)$ as well as the PDF of the corresponding phase processes $\Theta(t)$.

3.1 PDF of MLSS processes

The joint PDF $p_{\Xi\Theta}(x,\theta;t)$ of the MLSS process $\Xi(t)$ and the corresponding phase process $\Theta(t)$ can be obtained by solving the integrals over the joint PDF $p_{\Xi\dot{\Xi}\Theta\dot{\Theta}}\left(x,\dot{x},\theta,\dot{\theta};t\right)$ according to (12), i.e.,

$$
\begin{aligned}
p_{\Xi\dot{\Xi}\Theta\dot{\Theta}}\left(x,\dot{x},\theta,\dot{\theta};t\right) &= \frac{x^2\, e^{-\frac{x^2}{2\sigma_1^2}} e^{-\frac{\left(\dot{m}_1^{(2)}(t)\right)^2+\left(\dot{m}_2^{(2)}(t)\right)^2}{2\beta_2}} e^{-\frac{\left(\dot{m}_1^{(3)}(t)\right)^2+\left(\dot{m}_2^{(3)}(t)\right)^2}{2\beta_3}} e^{-\frac{\left(\dot{m}_1^{(1)}(t)\right)^2+\left(\dot{m}_2^{(1)}(t)\right)^2}{2\beta_1}}}{(2\pi)^4\,\sigma_1^2\sigma_2^2\sigma_{A_{\text{MR}}}^2} \int_{-\infty}^{\infty}\int_{-\infty}^{\infty}\int_{-\infty}^{\infty}\int_{-\infty}^{\infty} dz_2\, dz_1\, dy_2\, dy_1 \\
&\times \frac{e^{-\frac{\left(z_1-m_1^{(3)}(t)\right)^2+\left(z_2-m_2^{(3)}(t)\right)^2}{2\sigma_{A_{\text{MR}}}^2}} e^{-\frac{\left(y_1+m_1^{(1)}(t)\right)^2+\left(y_2+m_2^{(1)}(t)\right)^2}{2\sigma_1^2}} e^{\frac{r\left(y_1+m_1^{(1)}(t)\right)\cos\theta+r\left(y_2+m_2^{(1)}(t)\right)\sin\theta}{\sigma_1^2}} e^{-\frac{\left(z_1^2+z_2^2\right)\left\{\dot{x}^2+(x\dot{\theta})^2\right\}}{2\left\{\beta_1\left(z_1^2+z_2^2\right)+\beta_3\left(y_1^2+y_2^2\right)+\beta_2\left(z_1^2+z_2^2\right)^2\right\}}}}{\beta_1\left(z_1^2+z_2^2\right)+\beta_3\left(y_1^2+y_2^2\right)+\beta_2\left(z_1^2+z_2^2\right)^2} \\
&\times e^{-\frac{y_1^2+y_2^2-2\left(y_2m_2^{(2)}(t)+y_1m_1^{(2)}(t)\right)z_1-2\left(y_2m_1^{(2)}(t)-y_1m_2^{(2)}(t)\right)z_2+\left\{\left(m_1^{(2)}(t)\right)^2+\left(m_2^{(2)}(t)\right)^2\right\}\left(z_1^2+z_2^2\right)}{2\sigma_2^2\left(z_1^2+z_2^2\right)}} e^{\frac{\beta_3\left(y_1^2+y_2^2\right)\left\{\left(\dot{m}_1^{(1)}(t)\right)^2+\left(\dot{m}_2^{(1)}(t)\right)^2\right\}}{2\beta_1\left\{\beta_1\left(z_1^2+z_2^2\right)+\beta_3\left(y_1^2+y_2^2\right)+\beta_2\left(z_1^2+z_2^2\right)^2\right\}}} \\
&\times e^{\frac{\beta_2^2\left(z_1^2+z_2^2\right)^2\left[\beta_3\left\{\left(\dot{m}_1^{(1)}(t)\right)^2+\left(\dot{m}_2^{(1)}(t)\right)^2\right\}+\beta_1\left\{\left(\dot{m}_1^{(3)}(t)\right)^2+\left(\dot{m}_2^{(3)}(t)\right)^2\right\}\right]+\beta_3\beta_1\left\{\left(\dot{m}_1^{(2)}(t)\right)^2+\left(\dot{m}_2^{(2)}(t)\right)^2\right\}\left[\beta_3\left(y_1^2+y_2^2\right)+\beta_1\left(z_1^2+z_2^2\right)\right]}{2\beta_3\beta_2\beta_1\left\{\beta_1\left(z_1^2+z_2^2\right)+\beta_3\left(y_1^2+y_2^2\right)+\beta_2\left(z_1^2+z_2^2\right)^2\right\}}} \\
&\times e^{\frac{z_2^2\left\{\dot{m}_1^{(2)}(t)\dot{m}_1^{(3)}(t)y_1+\dot{m}_2^{(2)}(t)\dot{m}_2^{(3)}(t)y_1+\dot{m}_2^{(2)}(t)\dot{m}_1^{(3)}(t)y_2-\dot{m}_1^{(2)}(t)\dot{m}_2^{(3)}(t)y_2-z_1\left(\dot{m}_1^{(1)}(t)\dot{m}_1^{(2)}(t)+\dot{m}_2^{(1)}(t)\dot{m}_2^{(2)}(t)\right)-z_2\left(\dot{m}_2^{(1)}(t)\dot{m}_1^{(2)}(t)-\dot{m}_1^{(1)}(t)\dot{m}_2^{(2)}(t)\right)\right\}}{\beta_1\left(z_1^2+z_2^2\right)+\beta_3\left(y_1^2+y_2^2\right)+\beta_2\left(z_1^2+z_2^2\right)^2}} \\
&\times e^{\frac{z_2\left\{2z_1\left(\dot{m}_2^{(2)}(t)\dot{m}_1^{(3)}(t)y_1-\dot{m}_1^{(2)}(t)\dot{m}_2^{(3)}(t)y_1-\dot{m}_1^{(2)}(t)\dot{m}_1^{(3)}(t)y_2-\dot{m}_2^{(2)}(t)\dot{m}_2^{(3)}(t)y_2\right)-z_1^2\left(\dot{m}_2^{(1)}(t)\dot{m}_1^{(2)}(t)-\dot{m}_1^{(1)}(t)\dot{m}_2^{(2)}(t)\right)+\left(\dot{m}_2^{(1)}(t)\dot{m}_1^{(3)}(t)-\dot{m}_1^{(1)}(t)\dot{m}_2^{(3)}(t)\right)y_1\right\}}{\beta_1\left(z_1^2+z_2^2\right)+\beta_3\left(y_1^2+y_2^2\right)+\beta_2\left(z_1^2+z_2^2\right)^2}} \\
&\times e^{\frac{z_1^2\left(\dot{m}_1^{(2)}(t)\dot{m}_2^{(3)}(t)y_2-\dot{m}_1^{(2)}(t)\dot{m}_1^{(3)}(t)y_1-\dot{m}_2^{(2)}(t)\dot{m}_2^{(3)}(t)y_1-\dot{m}_2^{(2)}(t)\dot{m}_1^{(3)}(t)y_2\right)-z_1\left(\dot{m}_1^{(1)}(t)\dot{m}_1^{(3)}(t)y_1+\dot{m}_2^{(1)}(t)\dot{m}_2^{(3)}(t)y_1+\dot{m}_2^{(1)}(t)\dot{m}_1^{(3)}(t)y_2-\dot{m}_1^{(1)}(t)\dot{m}_2^{(3)}(t)y_2\right)}{\beta_1\left(z_1^2+z_2^2\right)+\beta_3\left(y_1^2+y_2^2\right)+\beta_2\left(z_1^2+z_2^2\right)^2}} \\
&\times e^{-\frac{z_1^3\left(\dot{m}_1^{(1)}(t)\dot{m}_1^{(2)}(t)+\dot{m}_2^{(1)}(t)\dot{m}_2^{(2)}(t)\right)+\left\{\dot{m}_1^{(3)}(t)\left(y_2z_1-y_1z_2\right)+\dot{m}_2^{(3)}(t)\left(y_1z_1+y_2z_2\right)+\left(\dot{m}_2^{(1)}(t)+\dot{m}_2^{(2)}(t)z_1+\dot{m}_1^{(2)}(t)z_2\right)\left(z_1^2+z_2^2\right)\right\}(x\dot{\theta}\cos\theta+\dot{x}\sin\theta)}{\beta_1\left(z_1^2+z_2^2\right)+\beta_3\left(y_1^2+y_2^2\right)+\beta_2\left(z_1^2+z_2^2\right)^2}} \\
&\times e^{\frac{\left\{\dot{m}_2^{(3)}(t)\left(y_1z_2-y_2z_1\right)+\dot{m}_1^{(3)}(t)\left(y_1z_1+y_2z_2\right)+\left(\dot{m}_1^{(1)}(t)+\dot{m}_1^{(2)}(t)z_1-\dot{m}_2^{(2)}(t)z_2\right)\left(z_1^2+z_2^2\right)\right\}(\dot{x}\cos\theta-x\dot{\theta}\sin\theta)-\left\{\dot{m}_2^{(1)}(t)\dot{m}_2^{(3)}(t)+\dot{m}_1^{(1)}(t)\dot{m}_1^{(3)}(t)\right\}y_2z_2}{\beta_1\left(z_1^2+z_2^2\right)+\beta_3\left(y_1^2+y_2^2\right)+\beta_2\left(z_1^2+z_2^2\right)^2}} \\
&\times e^{\frac{\beta_1\left(z_1^2+z_2^2\right)\left\{\left(\dot{m}_1^{(3)}(t)\right)^2+\left(\dot{m}_2^{(3)}(t)\right)^2\right\}}{2\beta_3\left\{\beta_1\left(z_1^2+z_2^2\right)+\beta_3\left(y_1^2+y_2^2\right)+\beta_2\left(z_1^2+z_2^2\right)^2\right\}}}, \quad x\geq 0,\ |\dot{x}|<\infty,\ |\theta|\leq\pi,\ |\dot{\theta}|<\infty\,. \qquad (11)
\end{aligned}
$$

$$
p_{\Xi\Theta}(x,\theta;t) = \int_{-\infty}^{\infty}\int_{-\infty}^{\infty} p_{\Xi\dot{\Xi}\Theta\dot{\Theta}}\left(x,\dot{x},\theta,\dot{\theta};t\right) d\dot{\theta}\, d\dot{x} \qquad (12)
$$

for $x\geq 0$ and $|\theta|\leq\pi$. Substituting (11) in (12) results in the following expression

$$
\begin{aligned}
p_{\Xi\Theta}(x,\theta;t) &= \frac{x\, e^{\frac{x^2}{2\sigma_1^2}}}{(2\pi)^2\,\sigma_1^2\sigma_2^2\sigma_{A_{\text{MR}}}^2} \int_0^{\infty}\int_0^{\infty}\int_{-\pi}^{\pi}\frac{\omega}{\nu} e^{-\frac{(\omega/\nu)^2+\rho_2^2}{2\sigma_2^2}} e^{-\frac{\nu^2+\rho_{A_{\text{MR}}}^2}{2\sigma_{A_{\text{MR}}}^2}} e^{-\frac{g_1(\omega,\psi;t)}{2\sigma_1^2}} e^{-\frac{xg_3(\omega,\theta,\psi;t)}{\sigma_1}} I_0\left(\sqrt{g_2(\omega,\nu,\psi;t)}\right) \\
&\quad d\psi\, d\omega\, d\nu, \qquad x\geq 0,\ |\theta|\leq\pi \qquad (13)
\end{aligned}
$$

where

$$g_1(\omega, \psi; t) = \omega^2 + \rho_1^2 + 2\rho_1\omega\cos\left(\psi - 2\pi f_{\rho_1} t - \theta_{\rho_1}\right) \tag{14a}$$

$$g_2(\omega, \nu, \psi; t) = \left(\frac{\rho_2\omega}{\sigma_2^2\nu}\right)^2 + \left(\frac{\rho_{A_{\mathrm{MR}}}\nu}{\sigma_{A_{\mathrm{MR}}}^2}\right)^2 + \frac{2\rho_2\rho_{A_{\mathrm{MR}}}\omega}{\sigma_2^2\sigma_{A_{\mathrm{MR}}}^2}\cos\left[\psi - 2\pi\left(f_{\rho_2} f_{\rho_3}\right)t - \left(\theta_{\rho_2} + \theta_{\rho_3}\right)\right] \tag{14b}$$

$$g_3(\omega, \theta, \psi; t) = \frac{\rho_1\cos\left(\theta - 2\pi f_{\rho_1} t - \theta_{\rho_1}\right) + \omega\cos(\theta - \psi)}{\sigma_1}. \tag{14c}$$

In (13), $I_0(\cdot)$ is the zeroth-order modified Bessel function of the first kind [31].

The PDF $p_\Xi(x)$ of MLSS processes $\Xi(t)$ can be obtained by integrating (13) over θ in the interval $[-\pi, \pi]$. Hence,

$$p_\Xi(x) = \frac{x\, e^{-\frac{x^2}{2\sigma_1^2}}}{2\pi\,\sigma_1^2\sigma_2^2\sigma_{A_{\mathrm{MR}}}^2}\int_0^\infty\int_0^\infty d\nu\, d\omega\, \frac{\omega}{\nu} e^{-\frac{(\omega/\nu)^2+\rho_2^2}{2\sigma_2^2}} e^{-\frac{\nu^2+\rho_{A_{\mathrm{MR}}}^2}{2\sigma_{A_{\mathrm{MR}}}^2}} \times \int_{-\pi}^{\pi} d\psi\, e^{-\frac{g_4(\omega,\psi)}{2\sigma_1^2}} I_0\left(\frac{x}{\sigma_1^2}\sqrt{g_4(\omega,\psi)}\right) I_0\left(\sqrt{g_5(\omega,\nu,\psi)}\right) \tag{15}$$

for $x \geq 0$, where

$$g_4(\omega, \psi) = \omega^2 + \rho_1^2 + 2\rho_1\omega\cos(\psi) \quad \text{and}$$

$$g_5(\omega, \nu, \psi) = \left(\frac{\rho_2\omega}{\sigma_2^2\nu}\right)^2 + \left(\frac{\rho_{A_{\mathrm{MR}}}\nu}{\sigma_{A_{\mathrm{MR}}}^2}\right)^2 + \frac{2\rho_2\rho_{A_{\mathrm{MR}}}\omega}{\sigma_2^2\sigma_{A_{\mathrm{MR}}}^2}\cos(\psi). \tag{16a,b}$$

It is worth mentioning that the joint PDF $p_{\Xi\Theta}(x, \theta; t)$ in (13) is dependent on time t. Nevertheless, the PDF $p_\Xi(x)$ in (15) is independent of time t showing that MLSS processes $\Xi(t)$ are first order stationary.

The significance of the PDF $p_\Xi(x)$ lies in the fact that it can easily be utilized in the link level performance analysis of relay-based M2M communication systems. The bit error probability (BEP) or the symbol error probability (SEP) and the channel capacity are a few measures to evaluate the performance of communication systems at the link level. The evaluation of the BEP, the SEP, and the channel capacity usually requires the knowledge of the PDF of the signal-to-noise ratio (SNR). Thus, given the PDF $p_\Xi(x)$ of $\Xi(t)$, the computation of the PDF of the SNR is nothing but transformation of random variables.

Integrating (13) over x in the interval $[0, \infty)$ results in the following expression for the PDF $p_\Theta(\theta; t)$ of the phase process $\Theta(t)$

$$p_\Theta(\theta; t) = \int_0^\infty\int_0^\infty\int_{-\pi}^{\pi} d\psi\, d\omega\, d\nu\, \frac{\omega}{\nu}\frac{e^{-\frac{(\omega/\nu)^2+\rho_2^2}{2\sigma_2^2}} e^{-\frac{\nu^2+\rho_{A_{\mathrm{MR}}}^2}{2\sigma_{A_{\mathrm{MR}}}^2}}}{(2\pi)^2\,\sigma_2^2\sigma_{A_{\mathrm{MR}}}^2} e^{-\frac{g_1(\omega,\psi;t)}{2\sigma_1^2}} \times I_0\left(\sqrt{g_2(\omega, \nu, \psi; t)}\right) \times \left[1 + \sqrt{\frac{\pi}{2}} g_3(\omega, \theta, \psi; t)\, e^{\frac{1}{2}g_3^2(\omega,\theta,\psi;t)} \times \left\{1 + \Phi\left(\frac{g_3(\omega, \theta, \psi; t)}{\sqrt{2}}\right)\right\}\right], \quad |\theta| \leq \pi \tag{17}$$

where $g_1(\cdot, \cdot; t)$, $g_2(\cdot, \cdot, \cdot; t)$, and $g_3(\cdot, \cdot, \cdot; t)$ are defined in (14a), (14b), and (14c), respectively. In (17), $\Phi(\cdot)$ represents the error function [31, Eq. (8.250.1)]. From (17), it is obvious that the phase process $\Theta(t)$ is not strict sense stationary, because the density $p_\Theta(\theta; t)$ is a function of time t. This time dependency of the PDF $p_\Theta(\theta; t)$ is due to the Doppler frequency f_{ρ_i} of the LOS component $m^{(i)}(t)$ $(i = 1, 2, 3)$. However, for the special case when $f_{\rho_i} = 0$, $\rho_i \neq 0$ $(i = 1, 2, 3)$, the phase process $\Theta(t)$ becomes a first order stationary process.

3.2 CDF of MLSS processes

The CDF $F_{\Xi_-}(r)$ of MLSS processes $\Xi(t)$ can be obtained by using [28, Eqs. (4.1), (4.6), (4.16)]

$$F_{\Xi_-}(r) = \int_{-\infty}^{r} p_\Xi(x)\, dx = 1 - \int_r^\infty p_\Xi(x)\, dx, \quad r \geq 0 \tag{18}$$

where $p_\Xi(x)$ is the PDF as given by (15). Substituting (15) in (18), allows us to write the final expression of the CDF $F_{\Xi_-}(r)$ of MLSS processes $\Xi(t)$ as

$$F_{\Xi_-}(r) = 1 - \frac{1}{(2\pi)^2\,\sigma_2^2\sigma_{A_{\mathrm{MR}}}^2}\int_0^\infty\int_0^\infty\int_{-\pi}^{\pi} d\psi\, d\omega\, d\nu \times \frac{\omega}{\nu} e^{-\frac{(\omega/\nu)^2+\rho_2^2}{2\sigma_2^2}} e^{-\frac{\nu^2+\rho_{A_{\mathrm{MR}}}^2}{2\sigma_{A_{\mathrm{MR}}}^2}} \times Q_1\left(\frac{\sqrt{g_4(\omega,\psi)}}{\sigma_1}, \frac{r}{\sigma_1}\right) I_0\left(\sqrt{g_5(\omega, \nu, \psi)}\right) \tag{19}$$

for $r \geq 0$. In (19), $g_4(\cdot,\cdot)$ and $g_5(\cdot,\cdot,\cdot)$ are the functions defined in (16a,b), respectively, whereas $Q_m(a,b)$ is the generalized Marcum Q-function [30].

3.3 Mean value and variance of MLSS processes

The PDF of a stochastic process plays a vital role in characterizing the process. However, the information provided by the PDF can also be summarized with the help of the expected value (mean value) and the variance of the stochastic process. The expected value m_Ξ of MLSS processes $\Xi(t)$ can be obtained by substituting (15) in [28, Eq. (5.44)] and performing some mathematical manipulations, i.e.,

$$\begin{aligned} m_\Xi = {} & \sqrt{\frac{\pi}{2}} \frac{\sigma_1}{(2\pi)^2 \sigma_2^2 \sigma_{A_{\mathrm{MR}}}^2} \\ & \times \int_0^\infty \int_0^\infty \int_{-\pi}^{\pi} d\psi\, d\omega\, d\nu \frac{\omega}{\nu} e^{-\frac{(\omega/\nu)^2+\rho_2^2}{2\sigma_2^2}} e^{-\frac{\omega^2+\rho_{A_{\mathrm{MR}}}^2}{2\sigma_{A_{\mathrm{MR}}}^2}} e^{-\frac{1}{2}\left(\frac{g_4(\omega,\psi)}{2\sigma_1^2}\right)} \\ & \times \left\{ \left(1 + \frac{g_4(\omega,\psi)}{2\sigma_1^2}\right) I_0\left(\frac{g_4(\omega,\psi)}{4\sigma_1^2}\right) \right. \\ & \left. + \left(\frac{g_4(\omega,\psi)}{2\sigma_1^2}\right) I_1\left(\frac{g_4(\omega,\psi)}{4\sigma_1^2}\right) \right\} I_0\left(\sqrt{g_5(\omega,\nu,\psi)}\right) \end{aligned} \tag{20}$$

where $g_4(\cdot,\cdot)$ and $g_5(\cdot,\cdot,\cdot)$ are defined in (16a,b), respectively.

The difference of the mean power $E\{\Xi^2(t)\}$ and the squared mean value m_Ξ^2 of MLSS processes $\Xi(t)$ defines its variance σ_Ξ^2 [28, Eq. (5.61)], i.e.,$\sigma_\Xi^2 = E\{\Xi^2(t)\} - m_\Xi^2$. Note that $E\{\cdot\}$ is the expected value operator. Using (15) and [28, Eq. (5.67)], the mean power $E\{\Xi^2(t)\}$ of MLSS processes $\Xi(t)$ can be expressed as

$$\begin{aligned} E\{\Xi^2(t)\} = {} & \int_0^\infty x^2\, p_\Xi(x)\, dx \\ = {} & \frac{1}{(2\pi)\sigma_2^2\sigma_{A_{\mathrm{MR}}}^2} \int_0^\infty \int_0^\infty \frac{\omega}{\nu} e^{-\frac{(\omega/\nu)^2+\rho_2^2}{2\sigma_2^2}} e^{-\frac{\nu^2+\rho_{A_{\mathrm{MR}}}^2}{2\sigma_{A_{\mathrm{MR}}}^2}} \\ & \times \int_{-\pi}^{\pi} \left\{2\sigma_1^2 + g_4(\omega,\psi)\right\} \\ & \times I_0\left(\sqrt{g_5(\omega,\nu,\psi)}\right) d\psi\, d\omega\, d\nu. \end{aligned} \tag{21}$$

Thus, the variance σ_Ξ^2 of MLSS processes $\Xi(t)$ can be computed by using (21) and (20).

3.4 LCR of MLSS processes

The LCR of the received envelope of mobile fading channels is a measure to describe the average number of times the envelope crosses a certain threshold level r from up to down (or vice versa) per second. The LCR $N_\Xi(r)$ of MLSS processes $\Xi(t)$ can be obtained using [32]

$$N_\Xi(r) = \int_0^\infty \dot{x}\, p_{\Xi\dot{\Xi}}(r,\dot{x})\, d\dot{x} \tag{22}$$

where $p_{\Xi\dot{\Xi}}(x,\dot{x})$ is the joint PDF of the MLSS process $\Xi(t)$ and its corresponding time derivative $\dot{\Xi}(t)$ at the same time t. From (11), the joint PDF $p_{\Xi\dot{\Xi}}(x,\dot{x})$ can be obtained by integrating over the undesirable variables θ and $\dot{\theta}$, i.e.,

$$\begin{aligned} p_{\Xi\dot{\Xi}}(x,\dot{x}) = {} & \int_{-\pi}^{\pi} \int_{-\infty}^{\infty} p_{\Xi\dot{\Xi}\Theta\dot{\Theta}}(x,\dot{x},\theta,\dot{\theta};t)\, d\dot{\theta}\, d\theta, \\ & x \geq 0,\ |\dot{x}| < \infty. \end{aligned} \tag{23}$$

In (11), after performing the transformation of random variables from rectangular to polar coordinates, substituting the values of $m_k^{(i)}(t)$ as well as $\dot{m}_k^{(i)}(t)$ ($i = 1, 2, 3$ and $k = 1, 2$), and doing some lengthy computations, the joint PDF $p_{\Xi\dot{\Xi}}(x,\dot{x})$ results in the following expression

$$\begin{aligned} p_{\Xi\dot{\Xi}}(x,\dot{x}) = {} & \frac{x\, e^{-\frac{x^2}{2\sigma_1^2}}}{\sqrt{2\pi}\,(2\pi)^3 \sigma_1^2\sigma_2^2\sigma_{A_{\mathrm{MR}}}^2} \\ & \times \int_0^\infty \int_0^\infty \int_{-\pi}^{\pi} \int_{-\pi}^{\pi} \int_{-\pi}^{\pi} d\theta\, d\psi\, d\phi\, d\omega\, d\nu \frac{\omega e^{-\frac{g_4(\omega,\psi)}{2\sigma_1^2}}}{\sqrt{\boldsymbol{\beta}(\omega,\nu)}} e^{\frac{x g_6(\omega,\theta,\psi)}{\sigma_1^2}} e^{-\frac{g_7(\omega,\nu,\psi,\phi)}{2\sigma_2^2}} \\ & \times e^{-\frac{g_8(\nu,\phi)}{2\sigma_{A_{\mathrm{MR}}}^2}} e^{-\frac{1}{2} g_9(\omega,\nu,\theta,\psi,\phi)} e^{-\frac{\dot{x}^2\nu^2}{2\boldsymbol{\beta}(\omega,\nu)}} e^{-\frac{\dot{x}\nu}{\sqrt{\boldsymbol{\beta}(\omega,\nu)}} g_9(\omega,\nu,\theta,\psi,\phi)}, \\ & x \geq 0,\ |\dot{x}| < \infty \end{aligned} \tag{24}$$

where

$$\boldsymbol{\beta}(\omega,\nu) = \beta_1\nu^2 + \beta_3\omega^2 + \beta_2\nu^4 \tag{25a}$$

$$g_6(\omega,\theta,\psi) = \rho_1\cos(\theta) + \omega\cos(\theta-\psi) \tag{25b}$$

$$g_7(\omega,\nu,\psi,\phi) = (\omega/\nu)^2 - 2(\omega/\nu)\rho_2\cos(\psi-\phi) + \rho_2^2 \tag{25c}$$

$$g_8(\nu,\phi) = \nu^2 - 2\nu\rho_{A_{\mathrm{MR}}}\cos(\phi) + \rho_{A_{\mathrm{MR}}}^2 \tag{25d}$$

$$\begin{aligned} g_9(\omega,\nu,\theta,\psi,\phi) = {} & \frac{2\pi f_{\rho_2}\rho_2\nu^2\sin(\theta-\phi) + 2\pi f_{\rho_1}\rho_1\nu\sin(\theta)}{\sqrt{\boldsymbol{\beta}(w,\nu)}} \\ & + \frac{2\pi f_{\rho_3}\rho_{A_{\mathrm{MR}}}\omega\sin(\theta-\psi+\phi)}{\sqrt{\boldsymbol{\beta}(\omega,\nu)}}. \end{aligned} \tag{25e}$$

Substituting (24) in (22) and further doing some tedious mathematical manipulations, the LCR $N_{\Xi}(r)$ of MLSS processes $\Xi(t)$ can be expressed as

$$N_{\Xi}(r) = \frac{\sqrt{2\pi}\, r\, e^{-\frac{r^2}{2\sigma_1^2}}}{(2\pi)^4 \sigma_1^2 \sigma_2^2 \sigma_{A_{\mathrm{MR}}}^2} \int_0^{\infty}\int_0^{\infty}\int_{-\pi}^{\pi}\int_{-\pi}^{\pi}\int_{-\pi}^{\pi} d\theta\, d\psi\, d\phi \times \sqrt{\boldsymbol{\beta}(\omega,\nu)}\frac{\omega}{\nu^2} e^{\frac{r g_6(\omega,\theta,\psi)}{\sigma_1^2}} e^{-\frac{g_4(\omega,\nu)}{2\sigma_1^2}} e^{-\frac{g_7(\omega,\nu,\psi,\phi)}{2\sigma_2^2}} e^{-\frac{g_8(\nu,\phi)}{2\sigma_{A_{\mathrm{MR}}}^2}} \times \left[e^{-\frac{1}{2}g_9^2(\omega,\nu,\theta,\psi,\phi)} + \sqrt{\frac{\pi}{2}} g_9(\omega,\nu,\theta,\psi,\phi) \times \left\{ 1 + \Phi\left(\frac{g_9(\omega,\nu,\theta,\psi,\phi)}{\sqrt{2}} \right) \right\} \right] d\omega\, d\nu \tag{26}$$

where $g_4(\cdot,\cdot)$, $\boldsymbol{\beta}(\cdot,\cdot)$, $g_6(\cdot,\cdot,\cdot)$, $g_7(\cdot,\cdot,\cdot,\cdot)$, $g_8(\cdot,\cdot)$, and $g_9(\cdot,\cdot,\cdot,\cdot,\cdot)$ are defined in (16a,b) and (25a)–(25e), respectively.

3.5 ADF of MLSS processes

The ADF of mobile fading channels is a measure to quantify how long the received envelope remains in average below a certain threshold level r. The ADF $T_{\Xi_-}(r)$ of MLSS processes $\Xi(t)$ can be obtained from the ratio of the CDF $F_{\Xi_-}(r)$ and the LCR $N_{\Xi}(r)$ [32], i.e.,

$$T_{\Xi_-}(r) = \frac{F_{\Xi_-}(r)}{N_{\Xi}(r)}\,. \tag{27}$$

The ADF $T_{\Xi_-}(r)$ of MLSS processes $\Xi(t)$ can easily be computed by substituting (19) and (26) in (27).

Note that MLSS fading channels belong to the class of time-variant multipath propagation and fading channels. Such channels exhibit bursty error characteristics [33]. The fading channel often causes the signal to fall below a certain threshold noise level, which in turn results in error bursts. The error bursts produced as a consequence of fading can be combated by using interleaving techniques [33, 34] and coding techniques [35, 36]. The PDF $p_{\Xi}(x)$ of $\Xi(t)$ is insufficient to be utilized in developing robust interleaving and coding schemes, as it does not give any insight into the rate of fading. The statistical quantities such as the LCR $N_{\Xi}(r)$ and the ADF $T_{\Xi_-}(r)$ describe the fading behavior of MLSS processes $\Xi(t)$. Studies pertaining to the LCR $N_{\Xi}(r)$ and the ADF $T_{\Xi_-}(r)$ of $\Xi(t)$ are thus quite useful in the design as well as optimization of coding and interleaving schemes for M2M fading channels in the relay links in cooperative networks.

4 Special cases of MLSS channels

The MLSS fading channel model developed in Section 2 incorporates at least five other fading processes as special cases. These special cases include double Rice [19], double Rayleigh [9, 14], SLDS [22], SLSS [20, 21], and NLSS [20, 21] fading channels. In this section, we will discuss the conditions under which MLSS fading processes reduce to any of the embedded processes. Furthermore, in order to demonstrate the flexibility of the analytical expression presented in Section 3, the expressions for the PDF, CDF, and LCR of all the above mentioned processes are also presented in this section. The proofs for the reduction of the PDF of MLSS processes to that of the stochastic processes mentioned above are included in Appendices A–E.

4.1 The double Rice process

The double Rice process is obtained by removing the direct SMS-DMS transmission link and considering LOS propagation conditions in the SMS-MR-DMS transmission link [19]. Thus, under the consideration when $\mu_{\rho_1}^{(1)}(t) \to 0$, i.e., $\rho_1 = 0$ and $\sigma_1^2 \to 0$, and choosing without loss of generality $A_{\mathrm{MR}} = 1$, the MLSS process in (2) reduces to

$$\chi_{\rho}(t)\Big|_{\substack{\rho_1=0\\ A_{\mathrm{MR}}=1\\ \sigma_1^2\to 0}} = \mu_{\rho}^{(2)}(t)\,\mu_{\rho}^{(3)}(t)\,. \tag{28}$$

Note that even though the direct SMS-DMS transmission link is not present, still the transmitted signal is available at the DMS every second time slot according to the amplify-and-forward relay protocol considered. The absolute value of the stochastic process in (28) defines the double Rice process, i.e.,

$$\Xi(t)\Big|_{\substack{\rho_1=0\\ A_{\mathrm{MR}}=1\\ \sigma_1^2\to 0}} = \left|\chi_{\rho}(t)\Big|_{\substack{\rho_1=0\\ A_{\mathrm{MR}}=1\\ \sigma_1^2\to 0}}\right| = \left|\mu_{\rho}^{(2)}(t)\,\mu_{\rho}^{(3)}(t)\right|\,. \tag{29}$$

Substituting $\rho_1 = 0$ and $A_{\mathrm{MR}} = 1$ in (15), (19), and (26) and taking the limit $\sigma_1^2 \to 0$, reduce the PDF, LCR, and ADF of the MLSS processes to the following corresponding expressions for double Rice processes:

$$p_{\Xi}(x)\Big|_{\substack{\rho_1=0\\ A_{\mathrm{MR}}=1\\ \sigma_1^2\to 0}} = \frac{x}{\sigma_2^2\sigma_{A_{\mathrm{MR}}}^2}\int_0^{\infty}\frac{1}{\nu}\, e^{-\frac{(x/\nu)^2+\rho_2^2}{2\sigma_2^2}} e^{-\frac{\nu^2+\rho_{A_{\mathrm{MR}}}^2}{2\sigma_{A_{\mathrm{MR}}}^2}} \times I_0\left(\frac{x\rho_2}{\nu\sigma_2^2}\right) I_0\left(\frac{\nu\rho_{A_{\mathrm{MR}}}}{\sigma_{A_{\mathrm{MR}}}^2}\right) d\nu,\ x \geq 0 \tag{30}$$

$$F_{\Xi_-}(r)\Big|_{\substack{\rho_1=0\\A_{\mathrm{MR}}=1\\\sigma_1^2\to 0}} = 1-\int_0^{\infty}\frac{\nu}{\sigma^2_{A_{\mathrm{MR}}}}e^{-\frac{\nu^2+\rho^2_{A_{\mathrm{MR}}}}{2\sigma^2_{A_{\mathrm{MR}}}}}I_0\left(\frac{\nu\rho_{A_{\mathrm{MR}}}}{\sigma^2_{A_{\mathrm{MR}}}}\right)\times Q_1\left(\frac{\rho_2}{\sigma_2},\frac{r}{\nu\sigma_2}\right)d\nu\; r\geq 0 \tag{31}$$

$$\begin{aligned}N_{\Xi}(r)\Big|_{\substack{\rho_1=0\\A_{\mathrm{MR}}=1\\\sigma_1^2\to 0}} =& \frac{r}{(2\pi)^2\sqrt{2\pi}\sigma_2^2\sigma^2_{A_{\mathrm{MR}}}}\\ &\times\int_0^{\infty}\frac{1}{\nu^2}\sqrt{\beta_2\nu^4+\beta_3 r^2}e^{-\frac{(r/\nu)^2+\rho_2^2}{2\sigma_2^2}}e^{-\frac{\nu^2+\rho^2_{A_{\mathrm{MR}}}}{2\sigma^2_{A_{\mathrm{MR}}}}}\\ &\times\int_{-\pi}^{\pi}e^{\frac{(r/\nu)\rho_2\cos(\phi-\psi)}{\sigma_2^2}}\int_{-\pi}^{\pi}e^{\frac{\nu\rho_{A_{\mathrm{MR}}}\cos\phi}{\sigma^2_{A_{\mathrm{MR}}}}}e^{-\frac{1}{2}g^2_{10}(r,\nu,\phi,\psi)}\\ &\times\left(1+\sqrt{\frac{\pi}{2}}g_{10}(r,\nu,\phi,\psi)\,e^{\frac{1}{2}g^2_{10}(r,\nu,\phi,\psi)}\right.\\ &\left.\times\left\{1+\Phi\left(\frac{g_{10}(r,\nu,\phi,\psi)}{2}\right)\right\}\right)d\phi\,d\psi\,d\nu\end{aligned} \tag{32}$$

where

$$g_{10}(r,\nu,\phi,\psi)=\frac{2\pi f_{\rho_3}r\rho_3\sin(\phi-\psi)-2\pi f_{\rho_2}\nu^2\rho_2\sin\phi}{\sqrt{\beta_2\nu^4+\beta_3 r^2}}. \tag{33}$$

The proof of (30) can be found in Appendix A, whereas the proofs of (31) and (32) have been omitted for reasons of brevity. We notice that the results in (30)–(33) have first been presented in the study conducted for double Rice processes in [19].

4.2 The double Rayleigh process

Considering NLOS propagation conditions in the SMS-MR-DMS link, when there is no direct transmission link between the SMS and the DMS, a double Rayleigh process comes into play. Thus, substituting $\rho_2=\rho_3=0$ in (29), results in the double Rayleigh process

$$\Xi(t)\Big|_{\substack{\rho_1,\rho_2,\rho_3=0\\A_{\mathrm{MR}}=1\\\sigma_1^2\to 0}} = \Big|\chi_\rho(t)\Big|_{\substack{\rho_1,\rho_2,\rho_3=0\\A_{\mathrm{MR}}=1\\\sigma_1^2\to 0}}\Big| = |\mu^{(2)}(t)\,\mu^{(3)}(t)|. \tag{34}$$

Applying the same conditions mentioned above on (15), (19), and (26) allows us to obtain the PDF, CDF, and LCR of double Rayleigh processes as follows:

$$p_{\Xi}(x)\Big|_{\substack{\rho_1,\rho_2,\rho_3=0\\A_{\mathrm{MR}}=1\\\sigma_1^2\to 0}} = \frac{x}{\sigma_2^2\sigma^2_{A_{\mathrm{MR}}}}K_0\left(\frac{x}{\sigma_2\sigma_{A_{\mathrm{MR}}}}\right),\quad x\geq 0 \tag{35}$$

$$F_{\Xi_-}(r)\Big|_{\substack{\rho_1,\rho_2,\rho_3=0\\A_{\mathrm{MR}}=1\\\sigma_1^2\to 0}} = 1-\frac{r}{\sigma_2\sigma_3}K_1\left(\frac{r}{\sigma_2\sigma_3}\right)\; r\geq 0 \tag{36}$$

$$N_{\Xi}(r)\Big|_{\substack{\rho_1,\rho_2,\rho_3=0\\A_{\mathrm{MR}}=1\\\sigma_1^2\to 0}} = \frac{r}{\sqrt{2\pi}\sigma_2^2\sigma^2_{A_{\mathrm{MR}}}}\times\int_0^{\infty}\frac{\sqrt{\beta_3 r^2+\beta_2\nu^4}}{\nu^2}e^{-\frac{(r/\nu)^2}{2\sigma_2^2}}e^{-\frac{\nu^2}{2\sigma^2_{A_{\mathrm{MR}}}}}d\nu\,. \tag{37}$$

The proof of (35) can be found in Appendix B. The expressions presented in (35)–(37) can be found in the literature (see, e.g., [9, 14]).

4.3 The SLDS process

The MLSS fading process tends to the SLDS fading process if a LOS component is considered only in the direct transmission link from the SMS to the DMS, ignoring the scattered component of the link [22]. The stochastic process associated with SLDS processes can be expressed by substituting $\rho_2=\rho_3=0$, $A_{\mathrm{MR}}=1$, and taking the limit $\sigma_1^2\to 0$ in (2) as follows

$$\chi_\rho(t)\Big|_{\substack{\rho_2,\rho_3=0\\A_{\mathrm{MR}}=1\\\sigma_1^2\to 0}} = m^{(1)}(t)+\mu^{(2)}(t)\,\mu^{(3)}(t)\,. \tag{38}$$

The absolute value of the stochastic process in (38) defines the SLDS process, i.e.,

$$\begin{aligned}\Xi(t)\Big|_{\substack{\rho_2,\rho_3=0\\A_{\mathrm{MR}}=1\\\sigma_1^2\to 0}} &= \Big|\chi_\rho(t)\Big|_{\substack{\rho_2,\rho_3=0\\A_{\mathrm{MR}}=1\\\sigma_1^2\to 0}}\Big|\\ &= \left|m^{(1)}(t)+\mu^{(2)}(t)\,\mu^{(3)}(t)\right|.\end{aligned} \tag{39}$$

Substituting $\rho_2=\rho_3=0$, $A_{\mathrm{MR}}=1$, and taking the limit $\sigma_1^2\to 0$ in (15), (19), and (26), allows us to obtain the

PDF, CDF, and LCR of SLDS processes in the form [22]

$$p_{\Xi}(x)\Big|_{\substack{\rho_2,\rho_3=0\\ A_{\mathrm{MR}}=1\\ \sigma_1^2\to 0}} = \begin{cases} \dfrac{x}{\sigma_2^2\sigma_{A_{\mathrm{MR}}}^2} I_0\left(\dfrac{x}{\sigma_2\sigma_{A_{\mathrm{MR}}}}\right) K_0\left(\dfrac{\rho_1}{\sigma_2\sigma_{A_{\mathrm{MR}}}}\right), & x<\rho_1 \\ \dfrac{x}{\sigma_2^2\sigma_{A_{\mathrm{MR}}}^2} K_0\left(\dfrac{x}{\sigma_2\sigma_{A_{\mathrm{MR}}}}\right) I_0\left(\frac{\rho_1}{\sigma_2\sigma_{A_{\mathrm{MR}}}}\right), & x\ge\rho_1 \end{cases} \tag{40}$$

$$F_{\Xi_-}(r)\Big|_{\substack{\rho_2,\rho_3=0\\ A_{\mathrm{MR}}=1\\ \sigma_1^2\to 0}} = \begin{cases} \dfrac{r}{\sigma_2\sigma_3} K_0\left(\dfrac{\rho_1}{\sigma_2\sigma_3}\right) I_1\left(\dfrac{r}{\sigma_2\sigma_3}\right), & r<\rho_1 \\ 1-\dfrac{r}{\sigma_1\sigma_2} I_0\left(\dfrac{\rho_1}{\sigma_2\sigma_3}\right) K_1\left(\dfrac{r}{\sigma_2\sigma_3}\right), & r\ge\rho_1 \end{cases} \tag{41}$$

$$\begin{aligned} N_{\Xi}(r)\Big|_{\substack{\rho_2,\rho_3=0\\ A_{\mathrm{MR}}=1\\ \sigma_1^2\to 0}} &= \frac{\sqrt{2\pi}\,r}{(2\pi)^2\sigma_2^2\sigma_{A_{\mathrm{MR}}}^2}\int_0^{\infty}\int_{-\pi}^{\pi} d\theta\,dv \\ &\times \frac{\sqrt{\beta_3\, g_{11}(r,\theta)+\beta_2 v^4}}{v^2} e^{-\frac{v^2}{2\sigma_{A_{\mathrm{MR}}}^2}} e^{-\frac{g_{11}(r,\theta)}{2v^2\sigma_2^2}} \\ &\times \left(e^{-\frac{1}{2}g_{12}^2(v,\theta)}+\sqrt{\frac{\pi}{2}}\,g_{12}(v,\theta)\right. \\ &\times \left.\left\{1+\Phi\left(\frac{g_{12}(v,\theta)}{\sqrt{2}}\right)\right\}\right) \end{aligned} \tag{42}$$

respectively, where

$$g_{11}(r,\theta)=r^2+\rho_1^2-2r\rho_1\cos\theta \quad \text{and}$$

$$g_{12}(v,\theta)=\frac{2\pi f_{\rho_1}\,\rho_1\, v\sin\theta}{\sqrt{\beta_3\, g_{11}(r,\theta)+\beta_2 v^4}}\,. \tag{43a,b}$$

The proof of (40) is given in Appendix C.

4.4 The SLSS process

The MLSS process tends to the SLSS process if NLOS propagation conditions are assumed in the transmission link between the SMS and the DMS via the MR. Thus, for $\rho_2=\rho_3=0$ and $A_{\mathrm{MR}}=1$, (2) reduces to the stochastic process given by

$$\chi_{\rho}(t)\Big|_{\substack{\rho_2,\rho_3=0\\ A_{\mathrm{MR}}=1}} = \mu_{\rho}^{(1)}(t)+\mu^{(2)}(t)\,\mu^{(3)}(t)\,. \tag{44}$$

Taking the absolute value of the stochastic process in (44) is referred to as the SLSS process, i.e.,

$$\begin{aligned} \Xi(t)\Big|_{\substack{\rho_2,\rho_3=0\\ A_{\mathrm{MR}}=1}} &= \left|\chi_{\rho}(t)\Big|_{\substack{\rho_2,\rho_3=0\\ A_{\mathrm{MR}}=1}}\right| \\ &= \left|\mu_{\rho}^{(1)}(t)+\mu^{(2)}(t)\,\mu^{(3)}(t)\right|\,. \end{aligned} \tag{45}$$

The PDF, CDF, and LCR of SLSS processes can be obtained by substituting ρ_2, $\rho_3=0$ and $A_{\mathrm{MR}}=1$ in (15), (19), and (26), respectively, i.e.,

$$\begin{aligned} p_{\Xi}(x)\Big|_{\substack{\rho_2,\rho_3=0\\ A_{\mathrm{MR}}=1}} &= \frac{x}{2\pi\,\sigma_1^2\sigma_2^2\sigma_{A_{\mathrm{MR}}}^2}\int_0^{\infty}\int_{-\pi}^{\pi} d\theta\,d\omega\,\omega\, e^{-\frac{\omega^2}{2\sigma_1^2}} e^{-\frac{g_{11}(x,\theta)}{2\sigma_1^2}} \\ &\times K_0\left(\frac{\omega}{\sigma_2\sigma_{A_{\mathrm{MR}}}}\right) I_0\left(\frac{\omega}{\sigma_1^2}\sqrt{g_{11}(x,\theta)}\right),\ x\ge 0 \end{aligned} \tag{46}$$

$$\begin{aligned} F_{\Xi_-}(r)\Big|_{\substack{\rho_2,\rho_3=0\\ A_{\mathrm{MR}}=1}} &= 1-\frac{1}{(2\pi)\,\sigma_2^2\sigma_3^2\sigma_1^2}\int_0^{\infty} d\omega\,\omega\, e^{-\frac{\omega^2}{2\sigma_1^2}} \\ &\times K_0\left(\frac{\omega}{\sigma_2\sigma_3}\right)\int_{-\pi}^{\pi}\int_r^{\infty} d\theta\,dx\,x\, e^{-\frac{g_{11}(x,\theta)}{2\sigma_1^2}} \\ &\times I_0\left(\frac{\omega}{\sigma_1^2}\sqrt{g_{11}(x,\theta)}\right),\ r\ge 0 \end{aligned} \tag{47}$$

$$\begin{aligned} N_{\Xi}(r)\Big|_{\substack{\rho_2,\rho_3=0\\ A_{\mathrm{MR}}=1}} &= \frac{\sqrt{2\pi}r}{(2\pi)^2\sigma_1^2\sigma_2^2\sigma_{A_{\mathrm{MR}}}^2}\int_0^{\infty}\int_0^{\infty}\int_{-\pi}^{\pi} d\theta\,d\omega\,dv \\ &\times \frac{\omega}{v^2}\sqrt{\boldsymbol{\beta}(\omega,v)}\, e^{-\frac{v^2}{2\sigma_{A_{\mathrm{MR}}}^2}} e^{-\frac{\omega^2}{2\sigma_1^2}} e^{-\frac{(\omega/v)^2}{2\sigma_2^2}} e^{-\frac{g_{11}(r,\theta)}{2\sigma_1^2}} \\ &\times I_0\left(\frac{\omega}{\sigma_1^2}\sqrt{g_{11}(r,\theta)}\right)\left[e^{-\frac{1}{2}g_{13}^2(\omega,v,\theta)}+\sqrt{\frac{\pi}{2}}\,g_{13}(\omega,v,\theta)\right. \\ &\times \left.\left\{1+\Phi\left(\frac{g_{13}(\omega,v,\theta)}{\sqrt{2}}\right)\right\}\right] \end{aligned} \tag{48}$$

where

$$g_{13}(\omega,v,\theta)=\frac{2\pi f_{\rho_1}\,\rho_1\, v\sin\theta}{\sqrt{\boldsymbol{\beta}(\omega,v)}}\,. \tag{49}$$

The proof of (46) is given in Appendix D. The expressions for the PDF and CDF of the SLSS process presented in (46) and (47), respectively, can be found in the literature [20, 21]. However, the expression for the LCR of the SLSS process given in (48) is one of our side results.

4.5 The NLSS process

The NLSS process assumes NLOS propagation conditions in both the transmission links, i.e., the direct SMS-DMS link and the SMS-MR-DMS link. This implies that $\rho_1 = \rho_2 = \rho_3 = 0$ and $A_{\mathrm{MR}} = 1$. Substituting $\rho_1 = 0$ in (45) gives the NLSS process, i.e.,

$$\Xi(t)\Big|_{\substack{\rho_1,\rho_2,\rho_3=0\\ A_{\mathrm{MR}}=1}} = \Big|\chi_\rho(t)\Big|_{\substack{\rho_1,\rho_2,\rho_3=0\\ A_{\mathrm{MR}}=1}}\Big| = \left|\mu^{(1)}(t) + \mu^{(2)}(t)\,\mu^{(3)}(t)\right| . \tag{50}$$

The PDF, CDF, and LCR of NLSS processes can be derived from the PDF, CDF, and LCR of MLSS processes by solving (15), (19), and (26), respectively, for $\rho_1 = \rho_2 = \rho_3 = 0$ and $A_{\mathrm{MR}} = 1$, i.e.,

$$p_\Xi(x)\Big|_{\substack{\rho_1,\rho_2,\rho_3=0\\ A_{\mathrm{MR}}=1}} = \frac{x\,e^{-\frac{x^2}{2\sigma_1^2}}}{\sigma_1^2\sigma_2^2\sigma_{A_{\mathrm{MR}}}^2}\int_0^\infty \omega\, e^{-\frac{\omega^2}{2\sigma_1^2}} K_0\!\left(\frac{\omega}{\sigma_2\sigma_{A_{\mathrm{MR}}}}\right) \times I_0\!\left(\frac{\omega}{\sigma_1^2}x\right) d\omega,\ x \geq 0 \tag{51}$$

$$F_{\Xi_-}(r)\Big|_{\substack{\rho_1,\rho_2,\rho_3=0\\ A_{\mathrm{MR}}=1}} = 1 - \frac{1}{\sigma_2^2\sigma_3^2}\int_0^\infty \omega\, K_0\!\left(\frac{\omega}{\sigma_2\sigma_3}\right) \times Q_1\!\left(\frac{\omega}{\sigma_1}, \frac{r}{\sigma_1}\right) d\omega, \quad r \geq 0 \tag{52}$$

$$N_\Xi(r)\Big|_{\substack{\rho_1,\rho_2,\rho_3=0\\ A_{\mathrm{MR}}=1}} = \frac{\sqrt{2\pi}\,r\,e^{\frac{-r^2}{2\sigma_1^2}}}{(2\pi)^2\,\sigma_1^2\sigma_2^2\sigma_{A_{\mathrm{MR}}}^2}\int_0^\infty\int_{0-\pi}^{\infty\ \pi} d\theta\,\frac{\omega}{v^2} \times\sqrt{\boldsymbol{\beta}(\omega, v)}\,e^{-\frac{v^2}{2\sigma_{A_{\mathrm{MR}}}^2}} e^{-\frac{\omega^2}{2\sigma_1^2}} e^{-\frac{(\omega/v)^2}{2\sigma_2^2}} \times I_0\!\left(\frac{r\omega}{\sigma_1^2}\right) d\omega\, dv\,. \tag{53}$$

The proof of (51) is given in Appendix E. To the best of our knowledge, analytical expressions for the LCR of NLSS processes have not yet been published. However, the PDF and CDF of NLSS processes are well-studied functions (see, e.g., [20, 21]).

5 Numerical results

The purpose of this section is twofold. Firstly, to illustrate the important theoretical results by evaluating the expressions in (15), (17), (19), (26), and (27). Secondly, we will confirm the correctness of the theoretical results with the help of simulations. The concept of sum-of-sinusoids (SOS) [32, 37] was exploited to simulate the underlying uncorrelated Gaussian noise processes of the overall MLSS process. The motivation to select an SOS-based channel simulator is that such simulators are widely acknowledged to be simple but efficient to model mobile radio fading channels under isotropic scattering conditions [30]. In addition, the concept of SOS has found its application in the design of channel simulators for temporally correlated frequency-nonselective channels [30, 38], frequency-selective channels [39, 40], and space-selective channels [12, 41–43]. However, in order to reproduce the desired channel characteristics in simulations, a careful selection of the simulator parameters is essential. For this reason, several methods for an accurate computation of the model parameters of SOS simulators have been developed [39, 40, 44–47]. One such method for the parameter computation, which is referred to as the generalized method of exact Doppler spread (GMEDS_1) [48], has been employed in this work. Using the GMEDS_1, it is possible to generate any number of uncorrelated Gaussian waveforms without increasing the complexity of the channel simulator. Each Gaussian process $\mu^{(i)}(t)$ was simulated using $\mathrm{N}_1^{(i)} = 20$ and $\mathrm{N}_2^{(i)} = 21$, where $\mathrm{N}_1^{(i)}$ and $\mathrm{N}_2^{(i)}$ are the number of sinusoids required to simulate the inphase and quadrature components of $\mu^{(i)}(t)$, respectively. It has been shown in [30] that with $\mathrm{N}_l^{(i)} \geq 7$ where $l = 1, 2$, the simulated distribution of $\left|\mu^{(i)}(t)\right|$ closely approximates the Rayleigh distribution. The variance of the inphase and quadrature components of $\mu^{(i)}(t)$ is equal to $\sigma_i^2 = 1$ for $i = 1, 2, 3$, unless stated otherwise. The Doppler frequencies, i.e., $f_{\mathrm{SMS}_{\max}}$, $f_{\mathrm{MR}_{\max}}$, and $f_{\mathrm{DMS}_{\max}}$, were set to 91 Hz, 75 Hz, and 110 Hz, respectively. Whereas, the Doppler frequencies of the three LOS components, i.e., f_{ρ_1}, f_{ρ_2}, and f_{ρ_3}, were set to 166 Hz, 185 Hz, and 201 Hz, respectively. For simplicity, the amplitudes of the three LOS components ρ_1, ρ_2, and ρ_3 are assumed to be equal, i.e., $\rho_1 = \rho_2 = \rho_3 = \rho$ and the relay gain $A_{\mathrm{MR}} = 1$, unless stated otherwise.

In the following, the theory is verified for many different propagation scenarios and the results presented in Figs. 2–6 show a good fit between the analytical and simulation results. These results illustrate that the statistics of MLSS fading channels corresponding to various propagation scenarios vary in a wide range. This in turn leads to the fact that the proposed model is highly flexible, since we expect that its statistics can be fitted to measurement data.

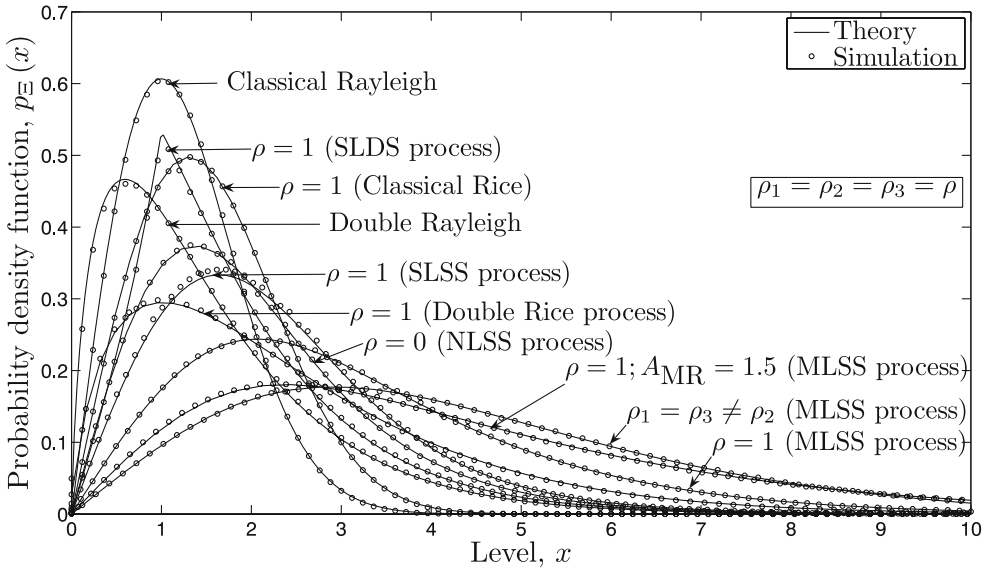

Fig. 2 A comparison of the PDF $p_{\Xi}(x)$ of the MLSS process $\Xi(t)$ with that of various other stochastic processes

The PDF $p_{\Xi}(x)$ of MLSS processes $\Xi(t)$ described by (15) is presented in Fig. 2 as well as the simulation results obtained by evaluating the statistics of the waveforms generated by using the SOS-based channel simulator. Figure 2 also shows several special cases of the PDF $p_{\Xi}(x)$ of MLSS processes $\Xi(t)$ that can be obtained by selecting appropriate values of ρ_1, ρ_2, ρ_3, and σ_{I}^2 in (15). The presented results show an excellent fitting between the analytical and simulation results. Studying the PDF $p_{\Xi}(x)$ of MLSS processes $\Xi(t)$ shows that the mean value m_{Ξ} and the variance σ_{Ξ}^2 of $\Xi(t)$ are greater than the mean values and the variances of the above mentioned processes for the same value of ρ. The same trend can be seen when different values of ρ_i $(i = 1, 2, 3)$ are selected. Furthermore, increasing the value of the relay gain A_{MR} causes an increase in the spread of the PDF $p_{\Xi}(x)$ of MLSS processes $\Xi(t)$. Similarly, Fig. 3 illustrates the theoretical results of the CDF $F_{\Xi_-}(r)$ of MLSS processes $\Xi(t)$ described by (19) along with the simulation results.

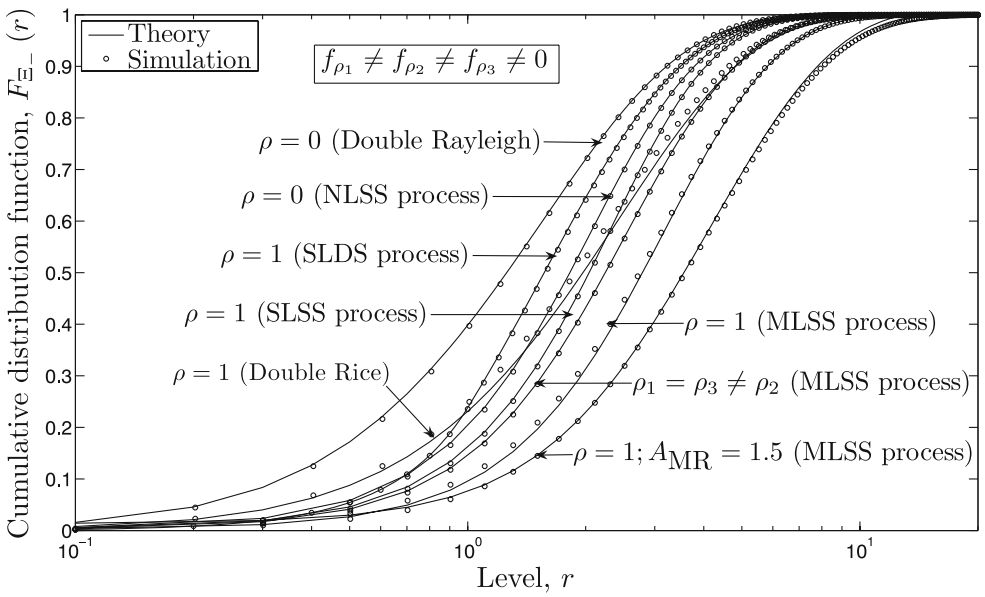

Fig. 3 A comparison of the CDF $p_{\Xi}(r)$ of the MLSS process $\Xi(t)$ with that of various other stochastic processes

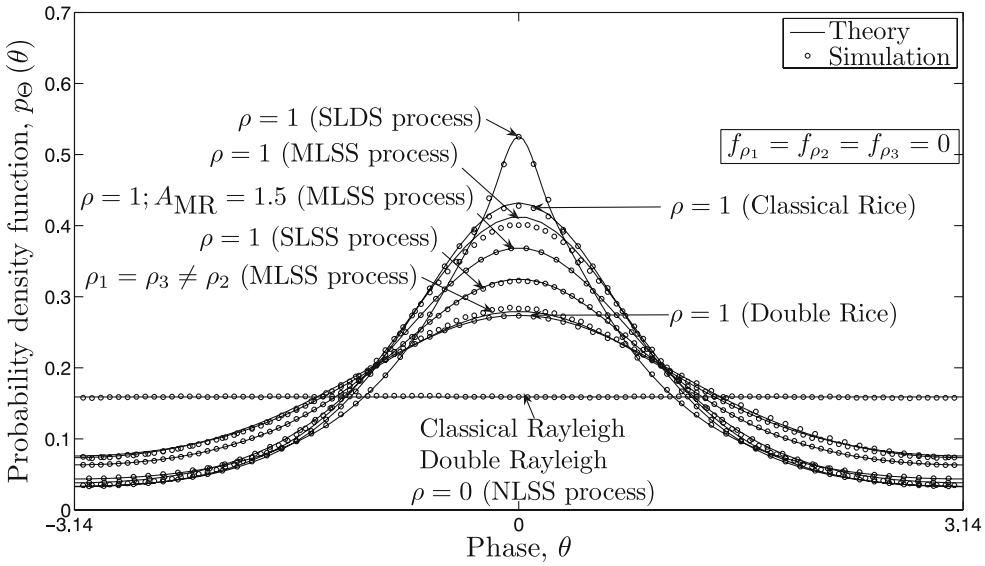

Fig. 4 A comparison of the PDF $p_\vartheta(\theta)$ of the phase of the MLSS process $\Theta(t)$ with that of various other stochastic processes

Figure 4 presents a comparison of the PDF $p_\Theta(\theta)$ of the phase process $\Theta(t)$ with that of the phase processes corresponding to classical Rayleigh, classical Rice, double Rayleigh, double Rice, SLDS, NLSS, and SLSS processes for $\rho = 1$. It should be noted that the results presented in Fig. 4 are valid for the case when f_{ρ_i} $(i = 1, 2, 3)$ is set to zero. It can be observed that the PDF of the phase process corresponding to the SLDS process has the smallest variance. The PDF $p_\Theta(\theta)$ follows the same trend in terms of the maximum value and the spread as that of the classical Rice process for the same value of ρ. Furthermore, it is interesting to note that for the phase process $\Theta(t)$ with ρ_i $(i = 1, 2, 3)$ being selected as $\rho_1 = \rho_3 = 0.5$ and $\rho_2 = 1$, the PDF $p_\Theta(\theta)$ is almost the same as that of the double Rice process for $\rho = 1$. In addition, conclusions can be drawn about the influence of the relay gain A_{MR} on the PDF $p_\Theta(\theta)$ of the phase process $\Theta(t)$ from Fig. 4 like, e.g.,

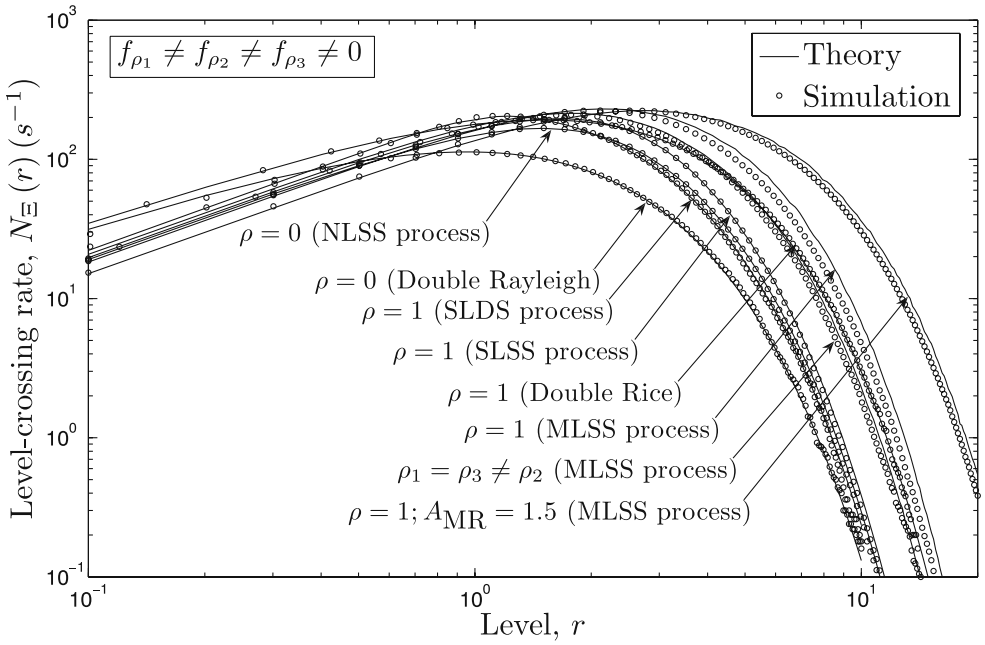

Fig. 5 A comparison of the LCR $N_\Xi(r)$ of the MLSS process $\Xi(t)$ with that of various other stochastic processes

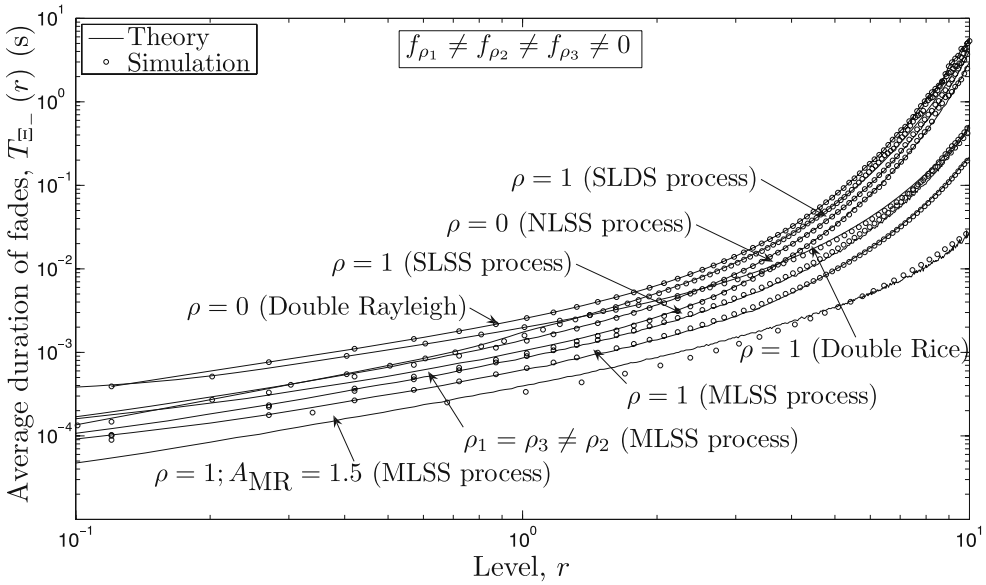

Fig. 6 A comparison of the ADF $T_{\Xi}(r)$ of the MLSS process $\Xi(t)$ with that of various other stochastic processes

as A_{MR} increases, the variance of the phase process $\Theta(t)$ increases.

The LCR $N_{\Xi}(r)$ of MLSS processes $\Xi(t)$ described by (26) is shown in Fig. 5. Like Figs. 2–4, Fig. 5 also presents a comparison of the LCR $N_{\Xi}(r)$ of MLSS processes $\Xi(t)$ with that of the LCR of several special cases, e.g., double Rayleigh, double Rice, SLDS, NLSS, and SLSS processes for some values of ρ. Studying the results presented in Fig. 5 shows that at low signal levels r, the LCR $N_{\Xi}(r)$ of MLSS processes $\Xi(t)$ is lower as compared to that of the special cases. This is in contrast to the behavior at medium and high levels, where the LCR $N_{\Xi}(r)$ of $\Xi(t)$ is higher than that of the LCR of the special cases. Furthermore, increasing the value of A_{MR} results in a decrease in the LCR $N_{\Xi}(r)$ at low signal levels r and in an increase in the LCR $N_{\Xi}(r)$ at medium and high signal levels.

The ADF $T_{\Xi_-}(r)$ of MLSS processes $\Xi(t)$ described by (27) is evaluated along with the simulation results in Fig. 6. For comparative purposes, the ADF of double Rayleigh, double Rice, SLDS, NLSS, and SLSS processes for some values of ρ is also presented in Fig. 6 along with the ADF $T_{\Xi_-}(r)$ of MLSS processes $\Xi(t)$. It can be observed that the ADF $T_{\Xi_-}(r)$ of MLSS processes $\Xi(t)$ is lower than the ADF of the mentioned stochastic processes. Furthermore, the decrease in the ADF $T_{\Xi_-}(r)$ as a consequence of an increase in the value of the relay gain A_{MR} is also visible in Fig. 6.

The qualitative description of the figures presented above is to put emphasis on the correctness of the derived analytical expressions. The quantitative analysis however is imperative to show how the channel and system parameters such as A_{MR}, ρ, f_{ρ}, etc. effect the statistics of the channel and to what extent. Thus, classifying the studied fading channels as NLOS M2M channels (i.e., double Rayleigh and NLSS channels) and LOS M2M channels (i.e., double Rice, SLDS, SLSS, and MLSS channels), we can conclude that LOS M2M channels have higher mean values and variances compared to NLOS M2M channels. Furthermore, the fading behavior of LOS M2M channels can be described by a higher LCR at higher signal levels (a lower LCR at lower signal levels) but a lower ADF when compared to that of NLOS M2M channels. The relay gain A_{MR} influences the statistics of both NLOS and LOS M2M fading channels in the same way, i.e., increasing A_{MR} increases the mean value, the variance, and the LCR of M2M fading channels. An increase in A_{MR} on the other hand decreases the ADF of the channels under discussion.

6 Conclusions

In this paper, we have proposed a new flexible M2M amplify-and-forward relay fading channel model under LOS conditions. The novelty in the model is that we are considering the LOS components in all transmission links, i.e., the direct link between the SMS and the DSM

as well as the two links via the MR. Thus, by analogy to multiple scattering radio propagation channels, we have introduced a new narrowband M2M channel referred to as the MLSS channel. The flexibility of the MLSS fading channel model comes from the fact that it includes several other channel models as special cases, e.g., double Rayleigh, double Rice, SLDS, NLSS, and SLSS channel models.

This paper presents a deep analysis pertaining to the statistical behavior of MLSS channels. Analytical expressions for the most important statistical properties like the mean, variance, PDF, CDF, LCR, and ADF of MLSS fading channels along with the PDF of the corresponding phase process are derived. The obtained theoretical results have complicated integral forms, which is inherent in the nature of the problem. However, that is not a serious drawback, since nowadays there are several efficient ways to solve multifold integrals numerically. Modern day computers and computer programs such as Matlab can give very accurate numerical results of integrals. Furthermore, using functions available in Matlab for numerical integration such as *trapz*, we managed to evaluate the derived analytical expressions with high accuracy and precision. An excellent fitting between the theoretical and simulation results confirms the correctness of the derived analytical expressions. It has been shown that under certain assumptions, the derived analytical expressions for the PDF, CDF, and LCR of MLSS processes reduce to the corresponding expressions of double Rayleigh, double Rice, SLDS, NLSS, and SLSS processes. The same is true for the ADF of MLSS processes as well as for the PDF of the corresponding phase processes. The presented results show that the PDF of MLSS processes has lower maximum value and higher spread in comparison to various special cases. Furthermore, at low signal levels, the LCR of MLSS processes is lower compared to that of several special cases. While, at medium and high signal levels, the LCR of MLSS processes is higher than that of the included special cases. A significant impact of the relay gain on different statistical properties of MLSS processes has also been observed. An increase in the relay gain decreases the maximum value of the PDF of MLSS processes and increases its spread. Similarly, an increase in the relay gain decreases the LCR of MLSS processes at low signal levels, whereas the LCR at medium and high signal levels increases. The opposite is true for the ADF of MLSS processes.

Our novel M2M channel model is useful for the system level performance evaluation of M2M communication systems in different M2M propagation scenarios. Furthermore, the theoretical results presented in this paper are beneficial for designers of the physical layer of M2M cooperative wireless networks. Based on our studies about the dynamics of MLSS fading channels, robust modulation, coding, and interleaving schemes can be developed and analyzed for M2M communication systems under LOS and NLOS propagation conditions.

Appendix A: Proof of (30)

For $\rho_1 = 0$, $A_{\mathrm{MR}} = 1$, and $\sigma_{\mathrm{I}}^2 \to 0$, (15) reduces to

$$p_{\Xi}(x)\Big|_{\substack{\rho_1=0\\A_{\mathrm{MR}}=1\\\sigma_{\mathrm{I}}^2\to 0}} = \frac{x}{2\pi\sigma_2^2\sigma_{A_{\mathrm{MR}}}^2}\int_0^{\infty}\int_0^{\infty}\int_{-\pi}^{\pi} d\psi\, d\nu\, d\omega \times \frac{\omega}{\nu} e^{-\frac{(\omega/\nu)^2+\rho_2^2}{2\sigma_2^2}} e^{-\frac{\nu^2+\rho_{A_{\mathrm{MR}}}^2}{2\sigma_{A_{\mathrm{MR}}}^2}} I_0\left(\sqrt{g_5(\omega,\nu,\psi)}\right) \times \underbrace{\lim_{\sigma_{\mathrm{I}}^2\to 0} \frac{e^{-\frac{x^2+\omega^2}{2\sigma_{\mathrm{I}}^2}}}{\sigma_1^2} I_0\left(\frac{x\omega}{\sigma_1^2}\right)}_{X_1} \tag{54}$$

for $x \geq 0$. Furthermore, using the asymptotic expansions of the zeroth-order modified Bessel function of the first kind $I_0(\cdot)$ [49, Sec. (7.23), Eq. (2)], allows us to write X_1 as

$$X_1 = \lim_{\sigma_{\mathrm{I}}^2\to 0} \frac{e^{-\frac{x^2+\omega^2}{2\sigma_{\mathrm{I}}^2}}}{\sigma_1^2} \frac{e^{\frac{x\omega}{\sigma_{\mathrm{I}}^2}}\sigma_1}{\sqrt{2\pi x\omega}} = \frac{1}{\sqrt{x\omega}} \lim_{\sigma_{\mathrm{I}}^2\to 0} \frac{e^{-\frac{x^2+\omega^2-2x\omega}{2\sigma_{\mathrm{I}}^2}}}{\sqrt{2\pi}\sigma_1} = \frac{1}{\sqrt{x\omega}}\delta(\omega - x)\ . \tag{55}$$

Substituting (55) in (54) gives

$$p_{\Xi}(x)\Big|_{\substack{\rho_1=0\\A_{\mathrm{MR}}=1\\\sigma_{\mathrm{I}}^2\to 0}} = \frac{x}{2\pi\sigma_2^2\sigma_{A_{\mathrm{MR}}}^2}\int_0^{\infty} d\nu\, \frac{1}{\nu} e^{-\frac{\nu^2+\rho_{A_{\mathrm{MR}}}^2}{2\sigma_{A_{\mathrm{MR}}}^2}} \int_{-\pi}^{\pi} d\psi \int_0^{\infty} d\omega \times \sqrt{\frac{\omega}{x}} e^{-\frac{(\omega/\nu)^2+\rho_2^2}{2\sigma_2^2}} I_0\left(\sqrt{g_5(\omega,\nu,\psi)}\right)\delta(\omega - x) \tag{56}$$

for $x \geq 0$. Applying the sifting property of the delta function [50] on (56) gives

$$p_{\Xi}(x)\Big|_{\substack{\rho_1=0\\A_{\mathrm{MR}}=1\\\sigma_1^2\to 0}} = \frac{x}{2\pi\sigma_2^2\sigma_{A_{\mathrm{MR}}}^2}\int_0^{\infty} d\nu\,\frac{1}{\nu}e^{-\frac{(x/\nu)^2+\rho_2^2}{2\sigma_2^2}}e^{-\frac{\nu^2+\rho_{A_{\mathrm{MR}}}^2}{2\sigma_{A_{\mathrm{MR}}}^2}} \times \underbrace{\int_{-\pi}^{\pi} I_0\left(\sqrt{g_5(x,\nu,\psi)}\right)d\psi}_{X_2},\ x \geq 0. \tag{57}$$

Numerical investigations show that it is possible to approximate X_2 in (57) as

$$X_2 = (2\pi)\, I_0\left(\frac{x\rho_2}{\nu\sigma_2^2}\right) I_0\left(\frac{\nu\rho_{A_{\mathrm{MR}}}}{\sigma_{A_{\mathrm{MR}}}^2}\right). \tag{58}$$

Thus, replacing (58) in (57) gives (30).

Appendix B: Proof of (35)

Substituting $\rho_1 = \rho_2 = \rho_3 = 0$ and $A_{\mathrm{MR}} = 1$ in (15), we can express $p_{\Xi}(x)\Big|_{\substack{\rho 1,\rho_2,\rho_3=0\\A_{\mathrm{MR}}=1}}$ as follows

$$p_{\Xi}(x)\Big|_{\substack{\rho 1,\rho_2,\rho_3=0\\A_{\mathrm{MR}}=1}} = \frac{x\, e^{-\frac{x^2}{2\sigma_1^2}}}{2\pi\sigma_1^2\sigma_2^2\sigma_{A_{\mathrm{MR}}}^2}\int_0^{\infty} d\omega\,\omega\, e^{-\frac{\omega^2}{2\sigma_1^2}} I_0\left(\frac{x\omega}{\sigma_1^2}\right) \times \underbrace{\int_0^{\infty}\frac{1}{\nu}e^{-\frac{(\omega/\nu)^2}{2\sigma_2^2}}e^{-\frac{\nu^2}{2\sigma_{A_{\mathrm{MR}}}^2}}\,d\nu}_{X_3=K_0\left(\frac{w}{\sigma_2\sigma_{A_{\mathrm{MR}}}}\right)} \underbrace{\int_{-\pi}^{\pi} d\psi}_{X_4=2\pi},\ x \geq 0 \tag{59}$$

where X_3 is obtained by using [31, Eq. (3.478.4)]. Taking the limit $\sigma_1^2 \to 0$, (59) can be written as

$$p_{\Xi}(x)\Big|_{\substack{\rho_1,\rho_2,\rho_3=0\\A_{\mathrm{MR}}=1\\\sigma_1^2\to 0}} = \frac{x}{\sigma_2^2\sigma_{A_{\mathrm{MR}}}^2}\int_0^{\infty} d\omega\,\omega K_0\left(\frac{\omega}{\sigma_2\sigma_{A_{\mathrm{MR}}}}\right) \times \lim_{\sigma_1^2\to 0}\frac{e^{-\frac{x^2+\omega^2}{2\sigma_1^2}}}{\sigma_1^2} I_0\left(\frac{\omega}{\sigma_1^2}x\right),\ x \geq 0. \tag{60}$$

Using the asymptotic expansions of the zeroth-order modified Bessel function of the first kind $I_0(\cdot)$ [49, Sec. (7.23), Eq. (2)], (60) can be expressed as

$$\begin{aligned} p_{\Xi}(x)\Big|_{\substack{\rho_1,\rho_2,\rho_3=0\\A_{\mathrm{MR}}=1\\\sigma_1^2\to 0}} &= \frac{x}{\sigma_2^2\sigma_{A_{\mathrm{MR}}}^2}\int_0^{\infty} d\omega\,\omega K_0\left(\frac{\omega}{\sigma_2\sigma_{A_{\mathrm{MR}}}}\right) \times \lim_{\sigma_1^2\to 0}\frac{e^{-\frac{x^2+\omega^2}{2\sigma_1^2}}}{\sigma_1^2}\frac{e^{\frac{x\omega}{\sigma_1^2}}\sigma_1}{\sqrt{2\pi x\,\omega}} \\ &= \frac{x}{\sigma_2^2\sigma_{A_{\mathrm{MR}}}^2}\int_0^{\infty} d\omega\sqrt{\frac{\omega}{x}}K_0\left(\frac{\omega}{\sigma_2\sigma_{A_{\mathrm{MR}}}}\right) \times \underbrace{\lim_{\sigma_1^2\to 0}\frac{e^{-\frac{x^2+\omega^2-2x\omega}{2\sigma_1^2}}}{\sqrt{2\pi}\sigma_1}}_{X_5},\ x \geq 0 \end{aligned} \tag{61}$$

where $X_5 = \delta(\omega - x)$ by definition of the delta function [51]. Thus, (61) can be written as

$$p_{\Xi}(x)\Big|_{\substack{\rho_1,\rho_2,\rho_3=0\\A_{\mathrm{MR}}=1\\\sigma_1^2\to 0}} = \frac{x}{\sigma_2^2\sigma_{A_{\mathrm{MR}}}^2}\int_0^{\infty} d\omega\sqrt{\frac{\omega}{x}}K_0\left(\frac{\omega}{\sigma_2\sigma_{A_{\mathrm{MR}}}}\right) \times\delta(\omega - x)\,,\ x \geq 0\,. \tag{62}$$

Applying the sifting property of the delta function [50] on (62), results in (35).

Appendix C: Proof of (40)

Substituting $\rho_2 = \rho_3 = 0$ as well as $A_{\mathrm{MR}} = 1$ and integrating (12) over θ from $-\pi$ to π allows us to write $p_{\Xi}(x)\Big|_{\substack{\rho_2,\rho_3=0\\A_{\mathrm{MR}}=1}}$ as

$$p_{\Xi}(x)\Big|_{\substack{\rho_2,\rho_3=0\\A_{\mathrm{MR}}=1}} = \frac{x}{(2\pi)^2\sigma_2^2\sigma_{A_{\mathrm{MR}}}^2}\int_0^{\infty}\int_{-\pi}^{\pi} d\theta\, d\omega \times \underbrace{\int_0^{\infty} d\nu\frac{\omega}{\nu}e^{-\frac{(\omega/\nu)^2}{2\sigma_2^2}}e^{-\frac{\nu^2}{2\sigma_{A_{\mathrm{MR}}}^2}}e^{-\frac{g_{11}(x,\theta)}{2\sigma_1^2}}}_{X_6=K_0\left(\frac{\omega}{\sigma_2\sigma_{A_{\mathrm{MR}}}}\right)} \times \underbrace{\int_{-\pi}^{\pi} e^{-\frac{\omega\{\rho_1\cos(\theta)+x\cos(\theta-\psi)\}}{\sigma_1^2}}d\psi}_{X_7=(2\pi)I_0\left(\frac{\omega}{\sigma_1^2}\sqrt{g_{11}(x,\theta)}\right)} \tag{63}$$

for $x \geq 0$. In (63), X_6 is evaluated using [31, Eq. (3.478.4)], whereas X_7 with the help of [31, Eq. (3.338.4)]. Taking the limit $\sigma_1^2 \to 0$ in (63), allows us to write

$$p_{\Xi}(x)\Big|_{\substack{\rho_2,\rho_3=0\\ A_{\mathrm{MR}}=1\\ \sigma_1^2\to 0}} = \frac{x}{2\pi\sigma_2^2\sigma_{A_{\mathrm{MR}}}^2}\int_0^{\infty}\int_0^{\infty}\int_{-\pi}^{\pi} d\theta\, dv\, d\omega \frac{\omega}{v} e^{-\frac{(\omega/v)^2}{2\sigma_2^2}} e^{-\frac{v^2}{2\sigma_{A_{\mathrm{MR}}}^2}} \times \lim_{\sigma_1^2\to 0} \frac{e^{-\frac{\omega^2}{2\sigma_1^2}} e^{-\frac{g_{11}(x,\theta)}{2\sigma_1^2}}}{\sigma_1^2} I_0\left(\frac{\omega}{\sigma_1^2}\sqrt{g_{11}(x,\theta)}\right) \tag{64}$$

for $x \geq 0$. Using the asymptotic expansions of the zeroth-order modified Bessel function of the first kind $I_0(\cdot)$ [49, Sec. (7.23), Eq. (2)], (64) can be expressed as

$$\begin{aligned} p_{\Xi}(x)\Big|_{\substack{\rho_2,\rho_3=0\\ A_{\mathrm{MR}}=1\\ \sigma_1^2\to 0}} &= \frac{x}{2\pi\sigma_2^2\sigma_{A_{\mathrm{MR}}}^2}\int_0^{\infty}\int_0^{\infty}\int_{-\pi}^{\pi} d\theta\, dv\, d\omega \frac{\omega}{v} e^{-\frac{(\omega/v)^2}{2\sigma_2^2}} e^{-\frac{v^2}{2\sigma_{A_{\mathrm{MR}}}^2}} \times \lim_{\sigma_1^2\to 0} \frac{e^{-\frac{\omega^2}{2\sigma_1^2}} e^{-\frac{g_{11}(x,\theta)}{2\sigma_1^2}}}{\sigma_1^2} \frac{e^{\frac{\omega}{\sigma_1^2}\sqrt{g_{11}(x,\theta)}}\sigma_1}{\sqrt{2\pi\omega}g_{11}(x,\theta)} \\ &= \frac{x}{2\pi\sigma_2^2\sigma_{A_{\mathrm{MR}}}^2}\int_0^{\infty}\int_0^{\infty}\int_{-\pi}^{\pi} d\theta\, dv\, d\omega \times \frac{\sqrt{\omega}}{v\, g_{11}(x,\theta)} e^{-\frac{(\omega/v)^2}{2\sigma_2^2}} e^{-\frac{v^2}{2\sigma_{A_{\mathrm{MR}}}^2}} \times \underbrace{\lim_{\sigma_1^2\to 0} \frac{e^{-\frac{\omega^2+\left(\sqrt{g_{11}(x,\theta)}\right)^2-2\omega\sqrt{g_{11}(x,\theta)}}{2\sigma_1^2}}}{\sqrt{2\pi}\sigma_1}}_{X_8} \end{aligned} \tag{65}$$

for $x \geq 0$. In (65), $X_8 = \delta(\omega - g_{11}(x,\theta))$ by definition of the delta function [51]. Thus, (65) can be written as

$$p_{\Xi}(x)\Big|_{\substack{\rho_2,\rho_3=0\\ A_{\mathrm{MR}}=1\\ \sigma_1^2\to 0}} = \frac{x}{2\pi\sigma_2^2\sigma_{A_{\mathrm{MR}}}^2}\int_0^{\infty}\int_0^{\infty}\int_{-\pi}^{\pi} d\theta\, dv\, d\omega \frac{\sqrt{\omega}}{v\, g_{11}(x,\theta)} \times e^{-\frac{(\omega/v)^2}{2\sigma_2^2}} e^{-\frac{v^2}{2\sigma_{A_{\mathrm{MR}}}^2}} \delta\left(\omega - \sqrt{g_{11}(x,\theta)}\right) \tag{66}$$

for $x \geq 0$. Applying the sifting property of the delta function [50] on (67) results in

$$p_{\Xi}(x)\Big|_{\substack{\rho_2,\rho_3=0\\ A_{\mathrm{MR}}=1\\ \sigma_1^2\to 0}} = \frac{x}{2\pi\sigma_2^2\sigma_{A_{\mathrm{MR}}}^2} \times \int_{-\pi}^{\pi} d\theta \underbrace{\int_0^{\infty} \frac{e^{-\frac{g_{11}^2(x,\theta)}{2\sigma_2^2 v^2}} e^{-\frac{v^2}{2\sigma_{A_{\mathrm{MR}}}^2}}}{v} dv}_{X_9 = K_0\left(\frac{\sqrt{g_{11}(x,\theta)}}{\sigma_2\sigma_{A_{\mathrm{MR}}}}\right)}, \quad x \geq 0\,. \tag{67}$$

where X_9 is evaluated using [31, Eq. (3.478.4)]. Thus, integrating (67) over θ from $-\pi$ to π results in the final expression given in (40).

Appendix D: Proof of (46)

Substituting $\rho_2 = \rho_3 = 0$ as well as $A_{\mathrm{MR}} = 1$ and integrating (12) over θ from $-\pi$ to π allows us to write $p_{\Xi}(x)\Big|_{\substack{\rho_2,\rho_3=0\\ A_{\mathrm{MR}}=1}}$ as

$$p_{\Xi}(x)\Big|_{\substack{\rho_2,\rho_3=0\\ A_{\mathrm{MR}}=1}} = \frac{x}{(2\pi)^2\sigma_2^2\sigma_{A_{\mathrm{MR}}}^2}\int_0^{\infty}\int_{-\pi}^{\pi} d\theta\, d\omega \times \underbrace{\int_0^{\infty} dv \frac{\omega}{v} e^{-\frac{(\omega/v)^2}{2\sigma_2^2}} e^{-\frac{v^2}{2\sigma_{A_{\mathrm{MR}}}^2}} e^{-\frac{g_{11}(x,\theta)}{2\sigma_1^2}}}_{X_{10} = K_0\left(\frac{\omega}{\sigma_2\sigma_{A_{\mathrm{MR}}}}\right)} \times \underbrace{\int_{-\pi}^{\pi} e^{-\frac{\omega\{\rho_1\cos(\theta)+x\cos(\theta-\psi)\}}{\sigma_1^2}} d\psi}_{X_{11} = (2\pi) I_0\left(\frac{\omega}{\sigma_1^2}\sqrt{g_{11}(x,\theta)}\right)} \tag{68}$$

for $x \geq 0$. In (68), X_{10} and X_{11} are evaluated using [31, Eq. (3.478.4)] and [31, Eq. (3.338.4)], respectively. Thus, replacing X_{10} and X_{11} in (68) results in (46).

Appendix E: Proof of (51)

Substituting $\rho_1 = \rho_2 = \rho_3 = 0$ and $A_{\mathrm{MR}} = 1$ in (15), we can express $p_{\Xi}(x)\Big|_{\substack{\rho 1,\rho_2,\rho_3=0\\ A_{\mathrm{MR}}=1}}$ as follows

$$p_{\Xi}(x)\Big|_{\substack{\rho 1,\rho_2,\rho_3=0\\ A_{\mathrm{MR}}=1}} = \frac{x\, e^{-\frac{x^2}{2\sigma_1^2}}}{2\pi\sigma_1^2\sigma_2^2\sigma_{A_{\mathrm{MR}}}^2}\int_0^{\infty} d\omega\, \omega\, e^{-\frac{\omega^2}{2\sigma_1^2}} I_0\left(\frac{x\omega}{\sigma_1^2}\right) \times \underbrace{\int_0^{\infty} \frac{1}{v} e^{-\frac{(\omega/v)^2}{2\sigma_2^2}} e^{-\frac{v^2}{2\sigma_{A_{\mathrm{MR}}}^2}}\, dv}_{X_{12}=K_0\left(\frac{w}{\sigma_2\sigma_{A_{\mathrm{MR}}}}\right)} \underbrace{\int_{-\pi}^{\pi} d\psi}_{X_{13}=2\pi},\ x \geq 0 \tag{69}$$

where X_{12} is evaluated using [31, Eq. (3.478.4)]. Thus, replacing X_{12} and X_{13} in (69) gives (51).

References

1. Akki AS, Haber F (1986) A statistical model of mobile-to-mobile land communication channel. IEEE Trans Veh Technol 35(1):2–7
2. Dohler M (2003) Virtual antenna arrays. PhD dissertation, King's College, London
3. Barbarossa S, Scutari G (2003) Cooperative diversity through virtual arrays in multihop networks. In: Proc. IEEE international conf. acoustics, speech, signal processing, vol 4. Hong Kong, China, pp 209–212
4. Sendonaris A, Erkip E, Aazhang B (2003) User cooperation diversity—Part I: system description. IEEE Trans Commun 51(11):1927–1938
5. Sendonaris A, Erkip E, Aazhang B (2003) User cooperation diversity—Part II: implementation aspects and performance analysis. IEEE Trans Commun 51(11):1939–1948
6. Laneman JN, Tse DNC, Wornell GW (2004) Cooperative diversity in wireless networks: efficient protocols and outage behavior. IEEE Trans Inf Theory 50(12):3062–3080
7. Andersen JB (2002) Statistical distributions in mobile communications using multiple scattering. In: Proc 27th URSI general assembly. Maastricht, Netherlands
8. Ercerg V, Fortune SJ, Ling J, Rustako AJ Jr, Valenzuela RA (1997) Comparison of a computer-based propagation prediction tool with experimental data collected in urban microcelluar environment. IEEE J Sel Areas Commun 15(4):677–684
9. Kovacs IZ, Eggers PCF, Olesen K, Petersen LG (2002) Investigations of outdoor-to-indoor mobile-to-mobile radio communication channels. In: Proc. IEEE 56th veh. technol. conf., VTC'02-Fall, vol 1. Vancouver BC, Canada, pp 430–434
10. Akki AS (1994) Statistical properties of mobile-to-mobile land communication channels. IEEE Trans Veh Technol 43(4):826–831
11. Maurer J, Fügen T, Wiesbeck W (2002) Narrow-band measurement and analysis of the inter-vehicle transmission channel at 5.2 GHz. In: Proc. IEEE 55th semiannual veh. technol. conf., VTC'02-Spring, vol 3. Birmingham, Alabama, pp 1274–1278
12. Pätzold M, Hogstad BO, Youssef N (2008) Modeling, analysis, and simulation of MIMO mobile-to-mobile fading channels. IEEE Trans Wirel Commun 7(2):510–520
13. Zajić AG, Stüber GL (2008) Space-time correlated mobile-to-mobile channels: modelling and simulation. IEEE Trans Veh Technol 57(2), 715–726
14. Patel CS, Stüber GL, Pratt TG (2006) Statistical properties of amplify and forward relay fading channels. IEEE Trans Veh Technol 55(1):1–9
15. Salo J, El-Sallabi HM, Vainikainen P (2006) Impact of double-Rayleigh fading on system performance. In: Proc. 1st IEEE int. symp. on wireless pervasive computing, ISWPC 2006. Phuket, Thailand. doi:0-7803-9410-0/10.1109/ISWPC.2006.1613574
16. Almers P, Tufvesson F, Molisch AF (2006) Keyhole effect in MIMO wireless channels: measurements and theory. IEEE Trans Wirel Commun 5(12):3596–3604
17. Shin H, Lee JH (2004) Performance analysis of space-time block codes over keyhole Nakagami-m fading channels. IEEE Trans Veh Technol 53(2):351–362
18. Sagias NC, Tombras GS (2007) On the cascaded Weibull fading channel model. J Franklin Inst 344:1–11 (Elsevier Ltd)
19. Talha B, Pätzold M (2007) On the statistical properties of double Rice channels. In: Proc. 10th international symposium on wireless personal multimedia communications, WPMC 2007. Jaipur, India, pp 517–522
20. Salo J, Salmi J, Vainikainen P (2005) Distribution of the amplitude of a sum of singly and doubly scattered fading radio signal. In: Proc. IEEE 61st semiannual veh. tech. conf., VTC'05-Spring, vol 1. Stockholm, Sweden, pp 87–91
21. Salo J, El-Sallabi HM, Vainikainen P (2006) Statistical analysis of the multiple scattering radio channel. IEEE Trans Antennas Propag 54(11):3114–3124
22. Talha B, Pätzold M (2007) On the statistical properties of mobile-to-mobile fading channels in cooperative networks under line-of-sight conditions. In: Proc. 10th international symposium on wireless personal multimedia communications, WPMC 2007. Jaipur, India, pp 388–393
23. Talha B, Pätzold M (2008) A novel amplify-and-forward relay channel model for mobile-to-mobile fading channels under line-of-sight conditions. In: Proc. 19th IEEE int. symp. on personal, indoor and mobile radio communications, PIMRC 2008. Cannes, France, pp 1–6. doi:10.1109/PIMRC.2008.4699733
24. Nabar RU, Bölcskei H, Kneubühler FW (2004) Fading relay channels: performance limits and space-time signal design. IEEE J Sel Areas Commun 22(6):1099–1109
25. Azarian K, Gamal HE, Schniter P (2005) On the achievable diversity-multiplexing tradeoff in half-duplex cooperative channels. IEEE Trans Inf Theory 51(12):4152–4172
26. Nabar RU, Bölcskei H (2003) Space-time signal design for fading relay channels In: Proc. IEEE globecom, vol 4. San Francisco, pp 1952–1956
27. Jakes WC (ed) (1994) Microwave mobile communications. IEEE, Piscataway
28. Papoulis A, Pillai SU (2002) Probability, random variables and stochastic processes, 4th edn. McGraw-Hill, New York
29. Simon MK (2002) Probability distributions involving gaussian random variables: a handbook for engineers and scientists. Kluwer Academic, Dordrecht
30. Pätzold M (2002) Mobile fading channels. Wiley, Chichester

31. Gradshteyn IS, Ryzhik IM (2000) Table of integrals, series, and products, 6th edn. Academic, New York
32. Rice SO (1945) Mathematical analysis of random noise. Bell Syst Tech J 24:46–156
33. Proakis J, Salehi M (2008) Digital communications, 5th edn. McGraw-Hill, New York
34. Tsie KY, Fines P, Aghvami AH (1992) Concatenated code and interleaver design for data transmission over fading channels. In: Proc. 9th international conference on digital satellite communications, ICDSC-9. Copenhagen, Denmark, pp 253–259
35. Biglieri E, Divsalar D, McLane PJ, Simon MK (1991) Introduction to trellis-coded modulation with applications. Macmillan, New York
36. Morris JM (1992) Burst error statistics of simulated Viterbi decoded BPSK on fading and scintillating channels. IEEE Trans Commun 40(1):34–41
37. Rice SO (1944) Mathematical analysis of random noise. Bell Syst Tech J 23:282–332
38. Patel CS, Stüber GL, Pratt TG (2005) Comparative analysis of statistical models for the simulation of Rayleigh faded cellular channels. IEEE Trans Commun 53(6):1017–1026
39. Höher P (1992) A statistical discrete-time model for the WSSUS multipath channel. IEEE Trans Veh Technol 41(4):461–468
40. Yip K-W, Ng T-S (1995) Efficient simulation of digital transmission over WSSUS channels. IEEE Trans Commun 43(12):2907–2913
41. Han J-K, Yook J-G, Park H-K (2002) A deterministic channel simulation model for spatially correlated Rayleigh fading. IEEE Commun Lett 6(2):58–60
42. Pätzold M, Youssef N (2001) Modelling and simulation of direction-selective and frequency-selective mobile radio channels. Int J Electron Commun AEÜ-55(6):433–442
43. Pätzold M, Hogstad BO (2004) A space-time channel simulator for MIMO channels based on the geometrical one-ring scattering model. Wirel Commun Mob Comput 4(7):727–737 (Special Issue on Multiple-Input Multiple-Output (MIMO) Communications)
44. Pätzold M, Killat U, Laue F (1996) A deterministic digital simulation model for Suzuki processes with application to a shadowed Rayleigh land mobile radio channel. IEEE Trans Veh Technol 45(2):318–331
45. Pätzold M, Killat U, Laue F, Li Y (1998) On the statistical properties of deterministic simulation models for mobile fading channels. IEEE Trans Veh Technol 47(1):254–269
46. Zheng YR, Xiao C (2002) Improved models for the generation of multiple uncorrelated Rayleigh fading waveforms IEEE Commun Lett 6(6):256–258
47. Pätzold M, Hogstad BO, Kim D (2007) A new design concept for high-performance fading channel simulators using set partitioning. Wirel Pers Commun 40(2):267–279
48. Pätzold M, Hogstad BO (2006) Two new methods for the generation of multiple uncorrelated Rayleigh fading waveforms. In: Proc. IEEE 63rd semiannual veh. tech. conf., VTC'06-Spring, vol 6. Melbourne, Australia, pp 2782–2786
49. Watson GN (1995) A treatise on the theory of Bessel functions, 2nd edn. Cambridge University Press, Bentley House, London
50. Oppenheim AV, Willsky AS, Hamid S (1996) Signals & systems, 2nd edn. Prentice-Hall, Inc., New Jersey
51. Papoulis A (1977) Signal analysis, 3rd edn. McGraw-Hill, Auckland